iEnergy

REVIEW

https://doi.org/10.23919/IEN.2024.0003

A review of the preparation process and anode stabilization strategies of Zn microbatteries

Xin Guo[1], Sajian Wu[3], Xiaojun Guo[1], Dexu Zheng[3], Yan Zhu[1], Jishuang Liu[3], Xinxin Xing[1], Haoxiang Zhang[1,2] ✉ and Shengzhong (Frank) Liu[1,2,4] ✉

ABSTRACT

As a burgeoning energy storage technology, Zn microbatteries (ZMBs) exhibit expansive potential for applications. This article initially presents a method for fabricating ZMBs utilizing interdigitated electrodes, employing advanced techniques such as 3D printing, screen printing, laser etching, and electrodeposition. These methodologies play a crucial role in mitigating anode-related issues, consequently enhancing battery performance. Subsequently, the challenges encountered by ZMBs anodes, including dendrite formation, corrosion passivation, hydrogen evolution, and Zn cycle exfoliation, are thoroughly examined. Lastly, a comprehensive strategy for stabilizing the anode is delineated, encompassing anode material selection, anode structure construction, interface engineering, and electrolyte optimization. In essence, the preparation and fine-tuning of ZMBs present ongoing challenges. With continued research and development efforts, it is anticipated that ZMBs will attain efficient, stable, and secure performance on the microscale, offering enduring and dependable energy solutions for applications in miniature electronic devices and wearable technology.

KEYWORDS

Zinc-ion, microbatteries, flexibility.

Energy and environmental concerns remain at the forefront of public attention. The inevitable depletion of various fossil and non-renewable energy sources underscores the urgency for new, clean[1], and renewable alternatives[2,3]. Wind energy[4], tidal energy[5], and solar energy have emerged as promising options[6]. Despite their appeal, these energy sources are significantly influenced by natural climate patterns, resulting in notable instability. Positioned as efficient electrochemical energy storage devices[7,8], batteries offer the dual advantages of high energy density and the ability to deliver continuous, stable electrical energy output. While lithium-ion batteries (LIBs) are extensively used across diverse fields due to their high energy density and low self-discharge rate[9], they grapple with challenges such as safety concerns, temperature limitations, and environmental issues, hampering their further advancement. In comparison, zinc-ion batteries (ZIBs) boast advantages such as abundant zinc resources, high energy density, robust safety profiles, and swift charge-discharge speeds, presenting a compelling alternative to traditional LIBs[10–12].

In the realm of emerging energy storage devices, ZMBs have garnered considerable attention, presenting notable advantages over traditional button-type ZIBs[13]. Their compact size and versatile shapes enable seamless adaptation to various space-intensive applications[14]. Additionally, ZMBs feature Zn nanosheet anodes with flexible properties[15], allowing for bending, folding, and embedding into flexible substrates. This inherent flexibility opens avenues for the development of wearable devices, flexible electronics, and other related fields. Moreover, these batteries showcase outstanding integration capabilities[16], facilitating the efficient assembly of multiple units to construct a high-performance energy storage system. This, in turn, enhances energy storage density and overall energy output, positioning ZMBs as promising candidates for commercial applications. In summary, as a novel energy storage device, ZMBs boast attributes such as small size, flexibility, integrability[15], cost-effectiveness, and environmental friendliness. With continuous technological advancements and the broadening scope of applications, ZMBs are poised to play a pivotal role in the future of energy storage.

This article aims to explore the reaction mechanism, manufacturing process, and challenges encountered by the anode of ZMBs. Concurrently, addressing the stability concerns of ZMBs anodes, the discussion will intricately cover four key aspects: anode material selection, porous structure construction, interface engineering, and electrolyte optimization.

1 Basic mechanism of ZMBs

The fundamental operating principle of ZMBs aligns with that of traditional ZIBs (refer to Figure 1). Both rely on the insertion/removal of Zn^{2+} between the positive and negative electrodes to store and release electrical energy. However, due to the limitations in size and thickness imposed on microbatteries (MBs), a specific selection of anode materials becomes imperative. Typically, the anode of ZMBs comprises metal oxides with robust chemical stability, such as zinc oxide and iron oxide. These oxides absorb Zn^{2+} during battery charging and release them during discharge. The cathode is typically constructed from materials

[1]Dalian National Laboratory for Clean Energy, Dalian Institute of Chemical Physics, Chinese Academy of Sciences, Dalian 116023, China; [2]Center of Materials Science and Optoelectronics Engineering, University of Chinese Academy of Sciences, Beijing 100049, China; [3]CNNP Optoelectronics Technology (Shanghai) Co., Ltd., Shanghai 201306, China; [4]Key Laboratory of Applied Surface and Colloid Chemistry, Ministry of Education, Shaanxi Key Laboratory for Advanced Energy Devices, Shaanxi Engineering Lab for Advanced energy Technology, Institute for Advanced Energy Materials, School of Materials Science and Engineering, Shaanxi Normal University, Xi'an 710119, China
Address correspondence to Haoxiang Zhang, haoxiangzhang@dicp.ac.cn; Shengzhong (Frank) Liu, szliu@dicp.ac.cn

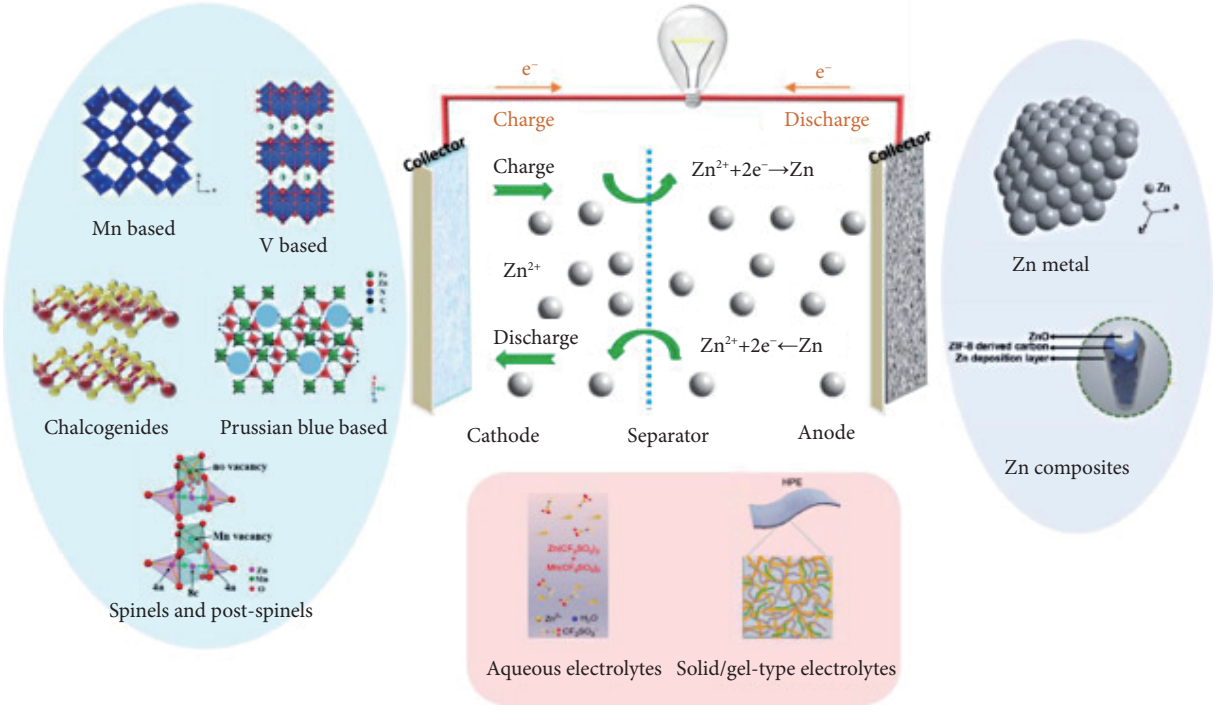

Figure 1 Working principle diagram of ZMBs. Reprinted with permission from Ref. [17], © 2019 Elsevier.

exhibiting high electrical conductivity and chemical stability, such as CdO and NiO. These materials effectively gather and transport electrons while providing ample space to accommodate migrating Zn^{2+}.

2 Preparation process of ZMBs

There are various common processes for the preparation of MBs, as summarized in Table 1. Specifically, the fabrication of ZMBs involves processes such as screen printing, 3D printing, laser etching, magnetron sputtering, electrodeposition, and spraying. To enhance the stability and cycle life of the electrode, proper surface treatment and coating are also applied[18,19]. Common ZMBs adopt structures like fiber[20,21], sheet[22,23], and interdigitated configurations. Among these, the interdigitated structure is preferred due to its higher energy density, faster reaction rate, superior cycle stability, and lower internal resistance[15]. In the electrode assembly, positive and anode materials are arranged on the same substrate in a interdigitated manner. Subsequently, the electrolyte is applied to cover the positive and anodes, followed by packaging and testing. Throughout this process, strict control over the flatness and positional accuracy of electrodes and separators is crucial to ensure the battery's stability and cycle life. Among them, the choice of substrate is also crucial. The selection of ZMB substrate must meet three key criteria: (1) Insulation: To ensure that the current is transmitted only through the electrolyte, the substrate must be insulated; otherwise, the battery will be directly short-circuited. (2) Stability: As the direct carrier of the battery, the substrate must exhibit good stability, meaning it will not react with the electrodes and electrolytes during tens of thousands of battery cycles. (3) Flexibility: Given the future targets of micro zinc-ion batteries as flexible wearables and microelectronic devices, flexible substrates can provide the necessary convenience.

2.1 Preparation of ZMBs by 3D printing

In recent years, 3D printing methods have gained widespread application in the energy storage equipment domain[42–45], particularly in the production of aqueous ZIBs[46,47]. This technology offers the advantages of cost-effectiveness, high efficiency, and the flexibility to manufacture electrodes and other components with intricate shapes and structures[48]. The integration of 3D printing technology enhances the flexibility of aqueous ZIBs design and significantly boosts manufacturing efficiency[49]. Leveraging 3D printing, electrode materials with unique shapes and structures can be easily produced, thereby enhancing the energy density and charge/discharge performance of batteries. Furthermore, this technology enables the creation of more intricate structures for MBs, contributing to lighter and more durable battery designs.

In the 3D printing electrode preparation process, the first step

Table 1 Comparison of various types of micro-battery preparation processes

Craft	Main technologies	Applicable size range	Advantages	Disadvantages	References
Lithography	Development technology	Micron and submicron level	High resolution	Complex operating steps and high environment requirements	[24–26]
Laser etching	Thermal effect	Micron and submicron level	High resolution and simple steps	Expensive and limited material selection	[27–29]
Screen printing	Orifice printing technology	Micron level	Easy processing and low cost	Lack of accuracy	[30–32]
Inkjet printing	Digital printing technology	Micron level	Personalized, thickness controllable	Suitable for small-scale production and low resolution	[33–36]
3D printing	Stacking technology	Micron and submicron level	High precision, flexible and controllable	Higher material property requirements	[37–41]

involves formulating ink suitable for 3D printing. The cathode electrode components comprise active materials, conductive carbon black, and polyvinylidene fluoride (PVDF), while anode materials primarily include Zn powder, polyvinylpyrrolidone (PVP), etc. Viscosity adjustment of the ink is crucial to ensure smooth 3D printing and the structural integrity of the solid material post-printing. Precision in 3D printing is achieved by adjusting the ratio of each ink component to meet viscosity requirements under different shear rates, facilitating high-precision preparation from ink to pattern. For instance, Zhu et al.[50] successfully prepared electrode materials with high precision and excellent shape fidelity through direct ink writing (DIW) 3D printing. This method can create electrodes of arbitrary shapes on various scales and was particularly successful in preparing high-rate alkali-based batteries. They controlled ink viscosity by adjusting different component ratios (i.e., ink composition: solid acrylic block copolymer, Zn powder, and a solvent composed of tetrahydrofuran and 2-butoxyethanol) (Figure 2(a), green area indicates optimal conditions), ensuring the ink meets shear strain resistance for shear thinning. Following high shear rate printing (Figure 2(b)), the ink's storage modulus can rapidly restore in a short time, achieving a solid–liquid–solid transition. Through this process, the 3D printing method efficiently realizes the printing of diverse patterns (Figure 2(c)).

In the realm of 3D printing technology, DIW and inkjet printing (IJP) stand out as two extensively employed methods. When it comes to crafting MBs, DIW is usually a priority compared to IJP. Renowned for its higher resolution and accuracy, DIW is particularly adept at printing smaller objects. For instance, Liu et al.[51] employed DIW to fabricate micro-flexible Zn-air batteries. The electrode ink comprises Co_3O_4 (cathode)/Zn powder (anode), graphene (G), Super-P (SP), and polyvinylidene fluoride (PVDF) mixed in *N*, *N*-dimethylformamide (DMF). The battery electrode inks are more intricate compared to traditional conductive battery electrode inks, given the addition of active ingredients like Co_3O_4. Co_3O_4 and Zn powder function as active materials, and also serves as the catalyst for oxygen reduction reaction (ORR) and oxygen evolution reaction (OER). While G and SP collaborate to form a robust three-dimensional network structure boasting ample mechanical strength and high electrical conductivity. Micron-sized Zn particles are deliberately chosen to facilitate functional electrochemical reactions. Utilizing 3D direct ink printing, multi-layer finger-shaped cathode air electrodes and anode Zn electrodes with full cells smaller than 2 cm^2 are precisely printed, controlling the minimum spacing between adjacent inter-finger electrodes to 100 μm. The battery uses a gel electrolyte and is suitable for a variety of flexible wearable technologies and has broad application prospects.

Moreover, Ma et al.[52] achieved the successful preparation of a Zn-CaVO battery boasting ultra-high capacitance and remarkable reversibility through the synergy of DIW and electrodeposition technology. In their meticulous preparation process (depicted in Figure 3), the DIW method was employed to print silver current collectors using silver-based ink. Concurrently, the cathode electrode was printed utilizing a mixed ink of calcium vanadate nanoribbons (CaVO NR), carbon nanotubes (CNTs), activated carbon (AB), and polyvinylidene fluoride (PVDF), with a mass ratio of 7:1:1:1. For the anode, they executed mixed ink printing of AB, reduced graphene oxide nanosheets (rGO NS), and PVDF, with a mass ratio of 7:2:1, and electrodeposited a Zn anode upon it. The stellar performance of the battery can be attributed to the favorable conditions provided by the two-dimensional rGO NS and CaVO NR for Zn attachment. Furthermore, the battery adopts a Cu^{2+} modified gel electrolyte, rendering it suitable for the demands of flexible wearable devices.

While 3D printing holds promise, challenges persist in the preparation of ZMBs, encompassing issues like low material utilization, inadequate structural precision, and suboptimal preparation efficiency. To address these challenges, several methods can be implemented: (1) Optimize the printing path and choose suitable materials, employing layered printing technology to minimize material waste. (2) Enhance printing accuracy and structural stability by refining the microbattery's structural design, incorporating porous structures to boost heat dissipation and mechanical

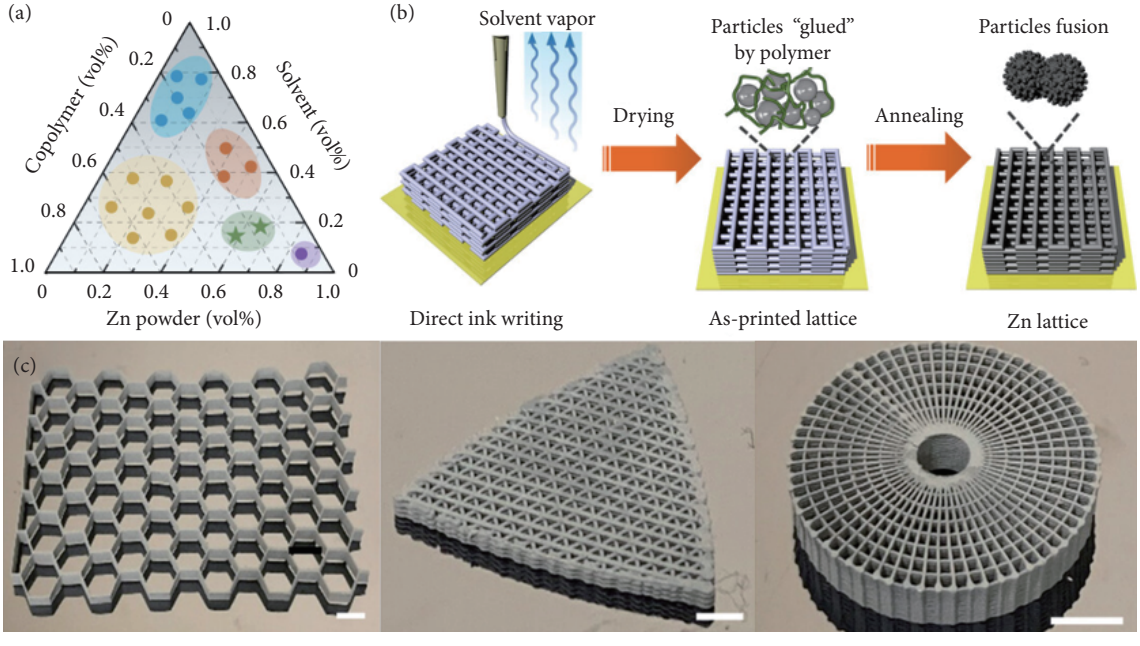

Figure 2 Schematic diagram of the 3D printed electrode. (**a**) Schematic diagram of the proportions of each component of 3D printing ink. (**b**) Schematic diagram of the 3D printing process. (**c**) 3D printing different shapes. Reprinted with permission from Ref. [50], © 2022 The Authors.

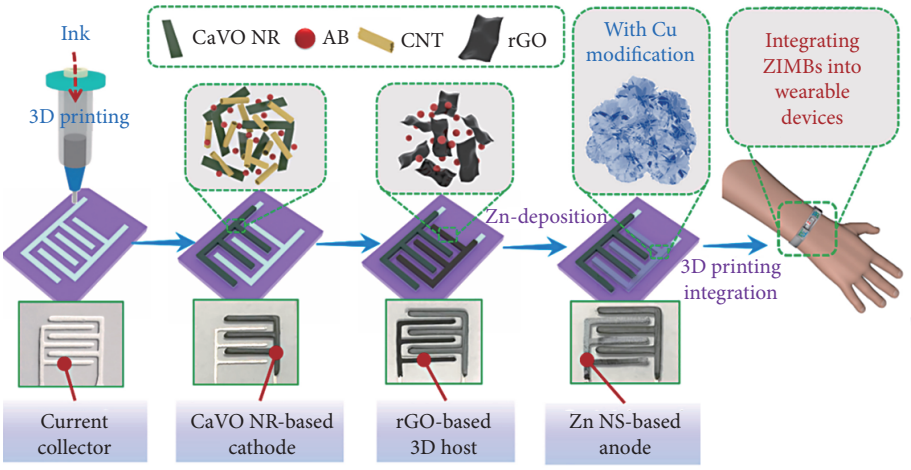

Figure 3 Schematic diagram of DIW Zn–CaVO MBs. Reprinted with permission from Ref. [52], © 2022 Elsevier.

strength[53]. (3) Improve preparation efficiency: Introduce automated printing equipment, such as robot arms, to reduce manual intervention and enhance production efficiency. (4) Improve the printing process: Utilize high-temperature sintering technology and other approaches to refine the printing process, thereby improving the performance and stability of ZMBs. (5) Optimize the electrode formula: By optimizing the electrode formula, potentially adding materials with higher electrochemical activity, such as Zn-based alloys and oxides, can improve the electrochemical performance of ZMBs. (6) Introduce auxiliary technologies: An innovative approach by Lu et al.[54] used a microfluidic-assisted 3D printing method, successfully creating a stable Zn-P anode by controlling the addition speed of each ink material. This method ingeniously managed the addition of electrode materials at varying rates, mitigating external interference for optimal outcomes.

2.2 Preparation of ZMBs by screen printing method

Printing technology, with a history spanning over a century, traces its roots back to ancient Chinese movable type printing[55], specifically porous printing. This method boasts attributes like cost-effectiveness, rapid molding, easy manufacturing, and broad versatility. By intricately designing meshes and applying specialized ink to form intricate patterns, the ink can be seamlessly transferred to nearly all substrates[56]. The operational mechanism of a screen printing machine involves a reciprocating process, wherein the mesh's opening area is filled against the resistance of the forward-moving scraper, followed by the reverse motion that imparts ink onto the substrate's surface under a specific scraper force. This facilitates the effortless creation of three-dimensional composite structures perpendicular to the substrate through successive back-and-forth printing steps. In recent years, the widespread adoption of screen printing in diverse miniaturized integrated circuits has substantially reduced their industrial-scale costs, propelling the practical application of this age-old printing technology[57].

Screen printing offers notable advantages in managing ink rheology and achieving precise pattern design, showcasing robust potential for extensive large-scale applications[58]. Its cost-effectiveness, ease of processing, and capability for mass production position screen printing as a highly practical method for the rapid fabrication of microelectronic devices. This method achieves precise control over performance, flexibility, and integration with printed microelectronics. Wang et al.[31] achieved successful preparation of Zn//MnO_2 MBs through screen printing, as illustrated in Figure 4. The process begins with the use of photoresist etching technology to etch the planar pattern of a full interdigitated electrode and two half interdigitated electrodes on the mold. The entire battery relies on a flexible polyethylene terephthalate (PET) substrate. Subsequently, a 4.2 μm thick metal-free current collector is printed on PET using pre-prepared graphene ink, utilizing full interdigitated electrodes as a template. MnO_2 ink is then employed to print on the half electrode of the metal-free current collector, using the half-interdigitated electrode plane pattern as a template to craft a 9.8 μm thick Zn//MnO_2 MBs cathode electrode. Finally, a 6.4 μm thick Zn anode electrode is printed on the other half of the electrode without a metal current collector, using Zn-based ink. The planar Zn//MnO_2 MBs prepared through this process exhibits exceptional flexibility in various bending states, without breaking or delaminating from the substrate. This printing technology is straightforward, efficient, and highly scalable, capable of producing intricate electrode patterns by modifying the template pattern.

While screen printing technology has long been a staple for electrode preparation, traditional manual manufacturing may present challenges, such as uneven Zn layer printing that can impact battery performance. Fortunately, the advent of specialized screen printing equipment has effectively addressed these issues. Zeng et al.[59] addressed concerns of unevenness and non-repeatability inherent in traditional manual operations by utilizing screen printing equipment manufactured by Shanghai Xuanting Screen Printing Equipment Co., Ltd. Employing this advanced device, they successfully fabricated Zn microhybrid supercapacitors for integration into light-charging flexible devices.

2.3 Preparation of ZMBs by laser etching

Laser etching[60], an industrial process employed for metal surface modification, additive manufacturing, and micromachining, offers high-precision processing capabilities, allowing precise control over the structure and size of MBs. Its key advantage lies in rapid processing speed, facilitating quick and effective preparation of MBs electrodes and other devices. Laser etching is versatile, suitable for processing various materials and complex shapes, including metals and polymers. This technology enables the design and manufacture of ZMBs in diverse shapes and sizes tailored to specific applications. Recent advancements involve the use of laser etching to create porous composite cathodes and conformal anodes with 3D structured electrodes. Li et al. employed full direct laser patterning (DLP) technology to fabricate customizable GO-Zn//rGO-MnO_2 MBs (Figure 5(a))[61]. Laser irradiation etched a Mn^{2+}-

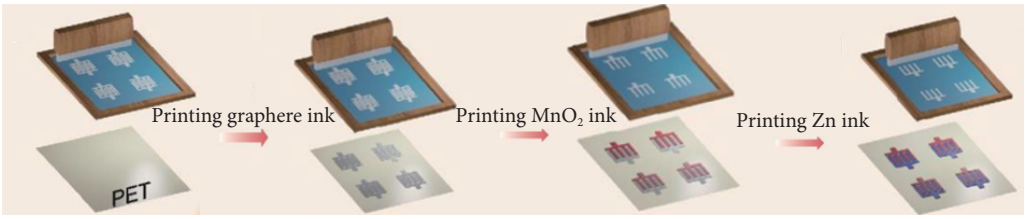

Figure 4 Schematic diagram of screen printing manufacturing of printed Zn//MnO_2 MBs. Reprinted with permission from Ref. [31], © 2019 The Author(s).

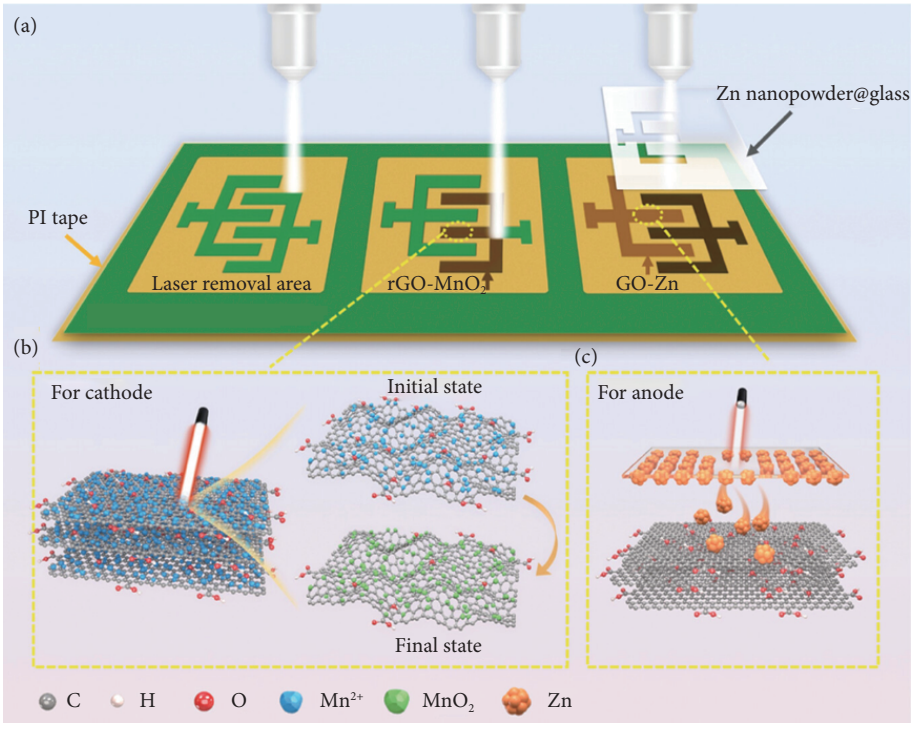

Figure 5 The laser etching process of GO-Zn//rGO-MnO_2. (a) Schematic diagram of laser etching GO-Zn//rGO-MnO_2. **(b)** Micrograph of laser etched rGO-MnO_2 cathode. **(c)** Micrograph of laser etched GO-Zn based anode. Reprinted with permission from Ref. [61], © 2023 Wiley.

graphene oxide (GO) film on graphite paper into an rGO-MnO_2 cathode electrode (Figure 5(b)), converting Mn^{2+} into MnO_2 nanometers through in-situ oxidation. This process generated oxygen vacancies, reducing GO and enhancing charge storage capabilities. Similarly, Zn nanoparticles were transferred from glass to GO film through laser thermal effects to prepare the GO/Zn anode electrode (Figure 5(c)). This approach enables template-free and efficient preparation of arbitrarily patterned electrodes while promoting the generation of oxygen vacancies within microelectrodes, enhancing active sites.

Typically, laser etching technology is not employed in isolation for the preparation of Zn microelectrodes; it often requires integration with other processes such as electrodeposition. In the investigation by Shi et al.[62], a multi-walled carbon nanotube-containing VO_2 film was initially obtained through filtration and stripping techniques, and a Zn film was prepared using the electrodeposition method. Subsequently, laser etching technology was utilized to precisely etch the interdigitated VO_2(B)-MWCNTs (multi-walled carbon nanotubes) cathode electrode and Zn anode electrode (Figures 6(a) and 6(b)). Finally, a Zn-VO_2 MBs was successfully crafted by covering it with $Zn(CF_3SO_3)_2$ gel electrolyte (Figure 6(c)). The laser engraving process enables the preparation of VO_2(B)-MWCNTs and Znnanosheet films with high capacitance and excellent rate capability in a simple, fast, and high-precision manner. In Wang et al.'s research[63], a CH@NC-LDH@NT core-shell electrode with a three-dimensional multi-level interconnection network structure was first prepared by electrodeposition, followed by cutting the forks using a laser etching process. The synergistic effect of the finger-shaped single cathode electrode, the unique core-shell structure, and the 3D porous interconnection network microelectrode offers higher capacity. The anode is prepared on a carbon nanotube base through the same process, preparing high-density rechargeable wearable alkaline Co-Zn MBs for smart textile applications. This unique core-shell structure design introduce a novel strategy for designing high-performance wearable textile microdevices.

However, when utilizing laser etching technology for the preparation of ZMBs, certain challenges may arise. Insufficient etching precision could result in suboptimal battery surface quality, and thermal effects during the etching process may adversely impact battery materials[64]. The high temperature of the laser, leading to laser ablation, might induce phase changes in the active material. To enhance etching accuracy, one can adjust laser parameters, including power and frequency, and implement an automated control system to ensure precision and consistency in the laser etching process[65]. Addressing concerns related to battery surface quality can be achieved through post-processing methods such as polishing and coating. Introducing a cooling system to the etching equipment to mitigate thermal effects during the process and incorporating materials resistant to thermal effects during the

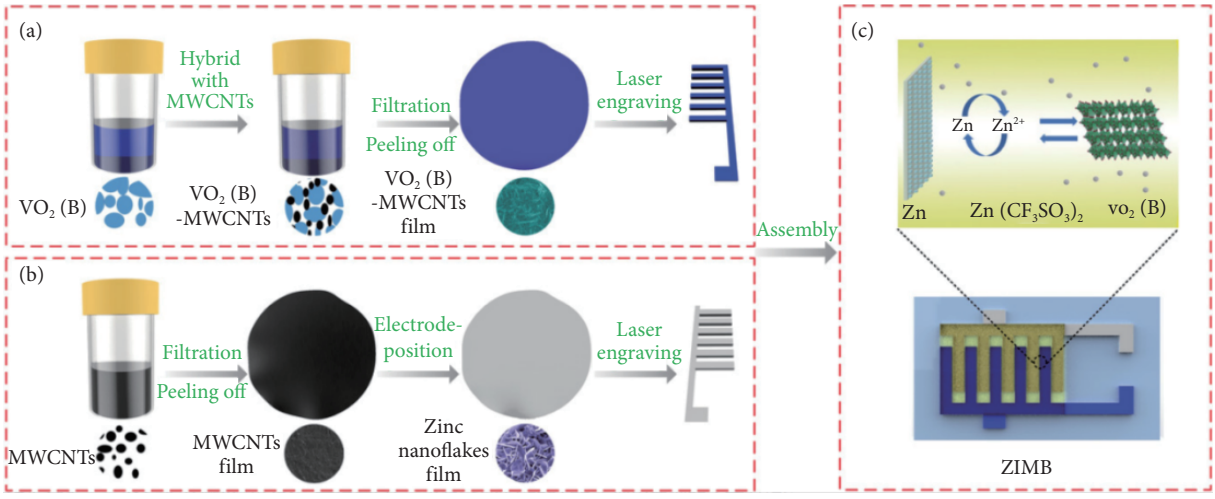

Figure 6 Schematic diagram of Zn-VO_2 MBs preparation. (**a**) VO_2(B)-MWCNTs cathode preparation process. (**b**) Zn anode preparation process. (**c**) Zn-VO_2 MBs assembly process. Reprinted with permission from Ref. [62], © 2019 Wiley.

electrode material preparation stage are effective strategies for resolving these issues.

2.4 Preparation of Zn microelectrode cells by electrodeposition

Electrodeposition technology stands out as one of the most extensively employed and well-established methods in battery preparation[66]. It has found widespread application, particularly in the fabrication of ZMBs[67]. Electrodeposition involves the deposition of metals or alloys from their compound solutions through electrochemical reactions[68,69]. This process serves as the foundation for various applications, including metal electrolytic smelting, electrolytic refining, electroplating, electroforming, and more. Typically conducted under specific electrolytic and operational conditions, utilizing double-electrode, three-electrode, and other systems, electrodeposition technology boasts advantages such as a high deposition rate, elevated purity, and enhanced deposition efficiency. These attributes contribute to its vast potential in the realm of battery preparation.

In this line of investigation, Sun et al.[70] employed an electrodeposition process to fabricate an interdigitated ZMBs with a finger width of 500 μm, a finger gap of 300 μm, and a total size of 4.5 mm × 4.5 mm. Illustrated in Figure 7, firstly, an Au current collector was crafted through a laser etching process. In a 0.1 M manganese acetate and 0.1 M sodium sulfate aqueous solution, MnO_2 cathode deposition was accomplished using cyclic voltammetry (CV) at a scan rate of 1.0 $mV{\cdot}s^{-1}$. (The Au interdigitated electrode was employed as the working electrode, platinum foil as the counter electrode, and Ag/AgCl electrode as the reference electrode.) The Zn anode was deposited at a constant current of 40 $mA{\cdot}cm^{-2}$, and its electrolyte consisted of 12.5 g $ZnSO_4$, 12.5 g Na_2SO_4, and 2.0 g H_3BO_3 and 100 mL deionized water. (The Au interdigitated electrode was employed as the working electrode, platinum foil as the counter electrode, and Ag/AgCl electrode as the reference electrode.) Finally, 2.0 M $ZnSO_4$ and 0.1 M $MnSO_4$ aqueous electrolytes were added dropwise. The resulting Zn-MnO_2 MBs exhibited an operating voltage as high as 1.74 V, showcasing promising applications in the miniaturized electronics industry.

In a similar vein, Wang et al. integrated 3D printing with electrodeposition technology[71] to ingeniously devise an economical, customizable, and user-friendly manufacturing approach, introducing a flexible conversion printing strategy. This innovative method initiates the process by crafting a reusable interdigitated pattern stamp through 3D printing of photopolymerized acrylate-based liquid resin. Subsequently, a Ni composite collector is generated on the 3D stamp via electrodeposition. Following this, MnO_2 cathode and Zn anode electrodes are fashioned through electrodeposition. The final step involves the assembly of the Zn-MnO_2 MBs utilizing specialized assembly tools.

Notably, in the investigation conducted by Dai et al.[72], they employed an innovative dual-electrode simultaneous deposition technology. Utilizing carbon nanotube paper (CNT) to sculpt a CNT double electrode featuring an interdigitated pattern and coupling it with a specialized electrodeposition method, they successfully fabricated a Zn anode electrode and a Br cathode electrode on carbon nanotubes simultaneously. Zn@CNT-Br_2@CNT microbattery were successfully prepared using this method. The key aspect of this technology lies in the electrolyte containing redox Zn^{2+} and Br^-. During the charging process, Zn^{2+} gains electrons and transforms into Zn, which deposits on the negative current collector to form the anode. Simultaneously, Br^- loses electrons and converts into Br_2, depositing on the positive current collector to create a cathode. Upon discharge, the deposits on the positive and anodes revert to corresponding positive and negative ions, dissolving in the electrolyte. This electrode preparation process offers significant advantages, requiring only an interdigitated current collector and a redox electrolyte. Bypassing the intricate processes of electrode coating, deposition, and cathode and anode mass matching, this method is considered an efficient and feasible approach to electrode preparation.

3 Problems with the anode of ZMBs

Throughout the charge-discharge cycle, ZMBs encounter not only the familiar challenges of anode dendrite formation, corrosion passivation, and hydrogen evolution witnessed in traditional ZIBs but also grapple with issues arising from their diminutive size and slender electrodes. There exists the potential for the Zn anode material to dislodge after numerous cycles during the charge-discharge process.

3.1 Anode dendrite problem

Much like other metal electrodes, the issue of dendrite formation commonly arises on the Zn anode electrodes[73–75]. This predicament primarily results from the non-uniform deposition of Zn onto the

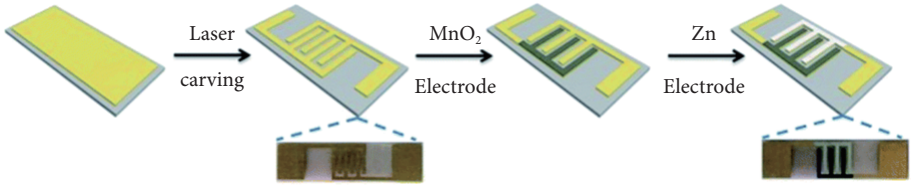

Figure 7 Schematic diagram of electrodeposition preparation of Zn-MnO_2 MB_s. Reprinted with permission from Ref. [70], © 2018 The Royal Society of Chemistry.

surface of Zn anodes. The lack of uniformity in deposition can be attributed to factors such as electric field distribution, ion distribution, and Zn nucleation distribution[76–78]. In the initial stages of the charge and discharge cycle in ZMBs, Zn would search for the active site on the electrode for nucleation growth and subsequently aggregate at these nucleation sites (Figure 8). However, with an increase in the number of cycles, the nucleation of Zn becomes uneven, influenced by external factors like the electric field on the electrode surface[79]. This non-uniform nucleation leads to a greater accumulation of Zn at uneven nucleation sites, setting off a detrimental cycle. Ultimately, dendrites may protrude into the internal separator of the battery, causing bulging or even resulting in a short circuit[80]. Addressing the challenge of Zn anode dendrites is imperative for ensuring the stability and safety of ZMBs and demands careful attention and resolution.

3.2 Corrosion passivation

Throughout battery operation, the anode surface of ZMBs undergoes corrosion and passivation reactions influenced by the characteristics of various electrolytes[81–83]. These reactions give rise to the formation of non-uniform passivation films, including byproducts like ZnO and $Zn(OH)_2$. The creation and stability of these passivation films are contingent on environmental conditions[84,85], such as electrolyte composition and temperature, as well as the properties of the anode surface.

Corrosion reaction:

$$Zn + 2OH^- \rightarrow Zn(OH)_2 + 2e^- \quad (1)$$

Under alkaline conditions, Zn reacts with OH^- to produce $Zn(OH)_2$ while simultaneously releasing electrons (Formula (1)).

Passivation reaction:

$$2Zn(OH)_2 + 2e^- \rightarrow 2ZnO + 2OH^- \quad (2)$$

This involves a reduction reaction where $Zn(OH)_2$ undergoes a transformation into ZnO and OH^- by capturing externally provided electrons (Formula (2)). Consequently, a mixed passivation film comprising OH^- and ZnO on the Zn anode's surface[86]. This film may not be uniformly distributed, resulting in surface roughening of the anode[82], and then leading to the uneven deposition of the dendrite. This exacerbates parasitic reactions, and the ZnO byproduct generated by this corrosion elevates the internal resistance of ZMBs. Moreover, it passivates surface activity to a large extent, ultimately contributing to capacity fading.

In neutral and weak acid electrolytes, corrosion and passivation are mainly associated with the precipitation of H_2[87]. The breakdown of H_2O and depletion of H^+ causes increased OH^- near the Zn anode and produces some insoluble byproducts that inactivate the anode. The formation of such insoluble products also increases the consumption of water and salt, thus shortening the battery life.

3.3 Hydrogen evolution problem

The hydrogen evolution reaction (HER) typically demonstrates subdued reaction characteristics in neutral and weakly acidic environments[88,89]. It typically occurs in alkaline electrolytes prior to Zn deposition[90]. The reaction can be represented as follows:

$$Zn + 2OH^- \rightarrow Zn(OH)_2 + 2e^- \quad (3)$$

$$H_2O + 2e^- \rightarrow H_2 + 2OH^- \quad (4)$$

In an alkaline environment, Zn metal reacts with OH^- in the alkaline solution, forming ZnO and H_2O while releasing electrons (Formula (3)). Subsequently, these electrons are reduced to hydrogen gas by H_2O (Formula (4)). The hydrogen evolution reaction (HER) can have several adverse effects on the battery: (1) Capacitance loss: The hydrogen evolution reaction leads to the formation of a foam-like structure of hydrogen on the electrode surface, causing a capacitance effect and reducing the actual capacity of the battery[91]. (2) Hydrogen evolution overpotential: The hydrogen evolution potential is lower than the redox potential of Zn, which means that the hydrogen evolution reaction consumes more electrolyte, which is not conducive to the normal operation of Zn[92]. (3) Energy loss: The hydrogen evolution reaction consumes the battery's charge, converting it into the chemical energy needed for hydrogen production. This results in a loss of chemical energy during discharge, reducing the available energy[93]. (4) Safety issues: The accumulation of hydrogen gas within the battery poses safety concerns, including the risk of leakage, overpressure, and explosion[94]. (5) Zinc loss: The hydrogen evolution reaction accelerates the corrosion of the Zn anode material, diminishing the battery's lifespan and cycle times[15]. There is a close connection between dendrites, corrosion passivation, and hydrogen evolution in ZMBs. Dendrite formation and hydrogen evolution: During the

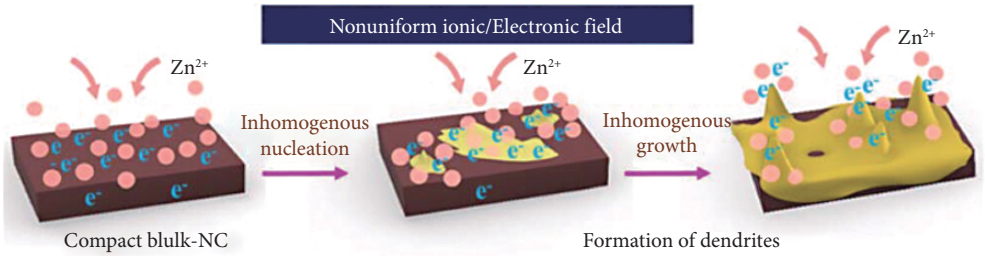

Figure 8 Schematic diagram of the dendrite phenomenon of Zn over cycle time. Reprinted with permission from Ref. [73], © 2022 Wiley.

charge and discharge process, when Zn^{2+} ions in the battery are reduced to Zn, dendrite formation may occur. These dendrites can serve as sites for Zn precipitation and promote the hydrogen evolution reaction. Therefore, dendrite formation can increase the rate of hydrogen evolution. Passivation corrosion and hydrogen evolution: Zn batteries may experience passivation corrosion after long-term use, wherein the Zn surface is oxidized to form an oxide film, hindering further corrosion. However, this passivation film also affects the hydrogen evolution reaction because it prevents the active centers on the electrode surface from contacting water molecules in the solution, thereby slowing down the rate of hydrogen evolution.

3.4 Problem of Zn anode exfoliation

The electrodes in prepared ZMBs are typically only tens of microns, sometimes even just several microns thick. Research shows that 10 μm is a critical value[95]. When the thickness of the Zn electrode is greater than 10 μm, although the problem of Zn exfoliation can be suppressed to a certain extent, it will seriously reduce the utilization rate of Zn. When the thickness of the Zn electrode is less than 10 μm, the Zn will fall off because the electrode is too thin. May become detached during circulation[96]. As the battery undergoes cycles, Zn on the negative electrode are progressively converted into Zn^{2+}, with some of these ions penetrating into the electrolyte. This penetration phenomenon occurs during both the discharging and charging processes. During discharge, Zn^{2+} gain electrons, transforming back into Zn; however, this process may lead to some Zn exfoliation from the negative electrode surface or penetrating into the electrolyte.Through continuous dissolution and deposition of electrode materials, the Zn negative electrode may gradually thin, and in extreme cases, a significant portion of it may exfoliation. This results in a substantial decline in the physical and chemical properties of the Zn electrode, potentially causing the battery to malfunction. This phenomenon not only escalates the cost associated with battery maintenance and replacement but also adversely affects the battery's lifespan and performance.

The issues mentioned above often initiate a vicious cycle, resulting in a continuous deterioration of battery performance that can ultimately lead to bulging, failure, and even pose a short circuit hazard. Consequently, to enhance the performance and lifespan of ZMBs, implementing an effective anode stabilization strategy is crucial. This strategy plays a pivotal role in ensuring the safety and stability of ZMBs.

4 Anode stabilization strategy for ZMBs

ZMBs encounter similar challenges to traditional ZIBs. The key distinction lies in their constraint by micro-battery size[95], demanding meticulous considerations in material selection and utilization. The primary focus is on the electrode material, structure and interface engineering of the ZMBs. When addressing structural concerns, the optimal choice for microbattery electrode construction is a three-dimensional porous framework[97,98]. Moreover, performance enhancements can be achieved through doping or alloying the Zn electrode with other elements[99]. Constructing a protective film on the electrode surface to isolate the interface between the anode and the electrolyte is an effective strategy to enhance ion transmission efficiency[100]. The recent introduction of gel electrolytes has played a crucial role in stabilizing the anode of ZMBs[101]. The single or double network structure of the gel electrolyte offers an efficient pathway for Zn^{2+} transmission.

4.1 Selection of anode materials

The selection of anode materials demonstrating excellent stability and reversibility during Zn^{2+} storage and release is pivotal. Commonly used anode materials encompass Zn powder, Zn-based materials (including alloys)[102–104], and carbon-based materials (such as carbon nanotubes and graphene)[105,106]. For instance, Dai et al.[72] utilized carbon nanotubes (CNT) to self-electrodeposit a Zn@CNT anode and Br_2@CNT cathode through a combined laser etching and double electrodeposition process, supplemented by an MPIBr gel electrolyte. The resulting Zn@CNT-Br_2@CNT battery featured an interdigitated pattern engraved on CNT paper. Opting for Zn-free CNTs as electrodes offers several advantages over direct Zn electrodes, such as: (1) Good conductivity[107]: Carbon nanotubes exhibit high conductivity, serving as effective channels for electron transmission. (2) High specific surface area[108,109]: With a nanometer size and unique structure, carbon nanotubes possess an extremely high specific surface area, facilitating increased contact with the electrolyte and enhancing reaction rates and electrochemical activity. (3) Mechanical strength[110]: Carbon nanotubes demonstrate excellent mechanical strength and durability, resisting friction and deformation. (4) Chemical stability[111]: Carbon nanotubes maintain high chemical stability under normal environmental conditions, resisting oxidation or corrosion.

These advantages render the CNT electrode a robust carrier for the insertion/extraction of Zn^{2+} during the battery cycle, eliminating the need for active material synthesis. The electrodeless nature of the battery requires only an interdigitated current collector and a redox-active electrolyte, eliminating challenges associated with coating or depositing cathodes and anodes on different microelectrodes. This approach avoids the cumbersome and time-consuming quality matching of cathode and anode processes, ultimately achieving the goal of anode protection.

Zhao et al.[112] devised a novel battery featuring a non-zinc anode. The cathode was formulated by blending VO_2 with multiwalled carbon nanotubes (MWCNTs), and the resulting VO_2-MWCNTs interdigitated electrode was created through laser etching. For the anode, an MXene-MWCNTs electrode was concocted by mixing MXene and TiS_2, complemented by a $ZnSO_4$-PAM gel electrolyte. The larger interlayer spacing of TiS_2 proves advantageous for the reversible diffusion of Zn^{2+}. Meanwhile, the layered structure of MXene inherently provides effective ion and electron transport pathways for Zn^{2+} and electrons. The cyclic voltammetry (CV) curve of MXene-TiS_2 reveals multi-step insertion during the charge and discharge process, signifying its ability to store/release more energy. Impressively, it sustains a capacity of 34.7 $mAh{\cdot}cm^{-2}$ at 100 °C, underscoring the excellent heat resistance of the ZMBs. MXene by itself has an elastic skeleton and a large specific area, which can provide abundant active sites for Zn deposition, but its weak Zn ophilic capacity[113]. Therefore, it is a wise strategy to hybridize MXene with other materials with high Zn affinity properties (such as carbon nanotubes and graphene) to effectively inhibit the growth and hydrogen evolution of Zn dendrite[114].

This battery technology employs unique non-zinc anodes known for their enhanced stability compared to traditional Zn anodes. It adeptly circumvents challenges such as dendrites, passivation, hydrogen evolution, and cyclic peeling often associated with Zn anodes, paving the way for significant advancements in battery technology. This innovative approach holds promising potential to effectively address the issues related to Zn anodes, thereby enhancing overall battery performance and lifespan. As technology continues to progress and application scenarios

expand, it is anticipated that this pioneering technology will assume a more pivotal role in the future battery market.

4.2 Porous electrode structure

Compared to non-zinc anodes, altering electrode characteristics by incorporating special nanomaterials has become a familiar approach. The careful construction of a three-dimensional skeleton microelectrode structure proves effective in promoting the uniform deposition of Zn^{2+} during cycling. This innovative structure prevents the collapse of the three-dimensional skeleton due to repeated insertion/detachment processes, ensuring the stability and durability of the electrode.

For instance, Lai et al.[28] devised a nickel nanocone array (NCA), growing directly on a conductive carbon film using the electrodeposition method. The resulting Zn@NCA anode and MnO_2@NCA cathode provide an outstanding capacity of 53.5 $\mu Ah \cdot cm^{-2} \cdot \mu m^{-1}$ at a 1 C rate, reaching a bulk energy density of 71.3 $\mu Wh \cdot cm^{-2} \mu m^{-1}$, with excellent cycling stability. Similarly, Liu et al.[98] utilized NCA to construct a unique three-dimensional microstructure, creating an excellent conductive framework and achieving remarkable results. The design of the three-dimensional skeleton intelligently anchors Zn-philic sites, actively promoting the uniform distribution of Zn^{2+} on the electrode. This not only enhances the energy density of the battery but also significantly extends its service life. Ma et al. introduced a design featuring a 3D printed Zn-philic *N*-doped hollow carbon nanotube (3DP-NHC) multi-channel body[115], aiming for an ideal dendrite-free Zn anode. The anode utilizes *N*-doped carbon nanotubes (NHCs) as the skeleton, obtained through acid etching, centrifugation, annealing, and 3D printing. Subsequent Zn electrodeposition yields the Zn@NHCs anode. The 3D-NHC structure with numerous porous channels and evenly distributed Zn-philic sites enhances ion diffusion rates during the charge and discharge cycles. It facilitates the uniform deposition of Zn, inhibits dendrites, and effectively prevents anode Zn exfoliation.

The three-dimensional skeleton structure also possesses the distinctive ability to facilitate the uniform penetration of electrolyte, undoubtedly enhancing the conductivity of the battery. This heightened conductivity helps diminish the internal resistance within the battery, ultimately improving its charge and discharge efficiency. And the Zn-doped carbon skeleton also facilitates the homogeneous deposition of Zn[116]. Moreover, the three-dimensional skeleton design increases the contact area between the electrode and the electrolyte. This augmented contact area further enhances the deposition efficiency of Zn^{2+} on the electrode, thereby optimizing battery performance.

4.3 Interface engineering

In addition to modifying the structure of the anode itself, various intricate reactions take place at the interface between the electrode and the electrolyte. Interface engineering plays a pivotal role in designing the negative electrode of ZMBs, allowing for optimization of the composition and structure of the interface to improve battery performance. The growth and side reactions of the Zn dendrite are associated with the electric field distribution and the diffusion behavior of Zn^{2+} highly correlated ions on the anode surface, and the nucleation barrier ion deposition of Zn^{2+}. Non-in situ formed protective layers (e. g., oxide[117,118], nitride[18], polymer, metal, carbon, and MXenes) can alter the surface properties of the bare Zn foil[119,120].This protective barrier must be chemically stable to resist potential reactions between the anode and electrolyte[121], while also maintaining excellent ionic conductivity to ensure optimal charge and discharge performance[122]. Therefore, enhancing the stability of the anode through interface engineering is a highly viable approach.

For instance, Zhai et al.[123] recently developed a fiber-shaped wearable ZIBs. They applied a nano-thin film of conductive carbon to the anode surface. This carbon layer not only enhances the uniform distribution of electrons at the reaction interface but also improves the electrochemical activity of the anode. The inclusion of the graphene-like carbon layer imparts good ductility and compressibility to the anode, along with abundant Zn nucleation sites, effectively suppressing anode dendrites and enhancing the stability and cycle life of the battery. This battery, in conjunction with the PEDOT:PSS@PANI cathode, exhibited outstanding performance, including a high capacity of 202.6 $mAh \cdot g^{-1}$, an energy density of 52.8 $mWh \cdot cm^{-3}$, and a peak power density of 2.4 $W \cdot cm^{-3}$, along with excellent cycle stability over 3,000 cycles.

Coating technology stands out as one of the commonly employed methods in interface engineering to address the stability issues of the anode[124]. Among the various corrosion-resistant technologies, the prevalent approach involves applying a polymer protective coating onto the anode surface[125]. While this protective layer effectively mitigates the corrosion of Zn anodes, it often impacts the plating/stripping dynamics of Zn on the anode surface, posing challenges in microscopic control. When implementing coating technology, a comprehensive assessment of its influence on anode stability and plating/stripping kinetics is necessary to ensure the rationality and efficacy of the coating. For instance, Zhu et al. successfully addressed the corrosion issue of ZMBs by employing polyimide coatings[126], resulting in a significant reduction in the capacity loss of ZIBs in aqueous electrolytes. The numerous carbonyl oxygen atoms in the polyimide coating can coordinate with Zn^{2+} in the electrolyte, forming a stable Zn layer. This coordination effectively diminishes the concentration gradient across the anode electrode/electrolyte interface, achieving rapid kinetics and low plating/stripping overpotential, thereby stabilizing the Zn anode. Another notable example is the work of He et al., who utilized atomic layer deposition (ALD) technology to create an ultrathin Al_2O_3 coating on the surface of the Zn plate[117]. This coating reduces the reactivity between the Zn electrode and the electrolyte during cycling. This enhances the corrosion resistance of Zn metal, inhibits dendrite formation during cycling, thereby reducing overpotential and impedance, and improving Zn plating/stripping reaction kinetics. This measure not only extends the cycle life but also reduces hysteresis voltage in the process.

Differing from the aforementioned coating technology applied at the interface between the electrode and the electrolyte, another approach involves integrating thin film technology between the current collector and the electrode. This technology shares similarities with the porous skeleton structure discussed in Section 5.2, utilizing materials such as copper molds, graphene films, among others. As an illustration, Zhou et al. cultivated a highly conductive, porous, large-area vertical graphene (VG) film on a titanium foil current collector through plasma-enhanced chemical vapor deposition (PECVD)[127]. Subsequently, the cathode and anode electrodes were electrodeposited onto the VG film, resulting in the fabrication of a Zn@VG//MnO_2@VG battery. The VG film introduces a uniformly distributed local electron flux, effectively promoting the uniform deposition/stripping of Zn. Functioning as a new connectivity network, VG facilitates ion transmission between the Zn anode and the MnO_2 cathode, augments charge transmission dynamics on the electrode, and enhances the adhesion of active materials to the current collector. Consequently, this

optimization of the electrode structure stability and the interface between the electrode and the electrolyte/current collector contributes to improved battery performance.

4.4 Electrolyte optimization measures

Currently, the mainstream electrolytes include liquid electrolytes, quasi-solid electrolytes (i.e., gel electrolytes), and all-solid electrolytes. Liquid electrolyte refers to an electrolyte that can decompose into ions in a solution or in a molten state, enabling electrical conduction[128]. All-solid electrolytes are batteries without liquid electrolytes, utilizing solid electrolytes between the positive and negative electrodes[129]. These solid ion conductors enable ion migration under an electric field, offering properties such as electrical conductivity, high chemical stability, and mechanical strength. In contrast, gel electrolytes, although sacrificing some mechanical strength, provide flexibility and deformability, allowing adaptation to various designs. This enhances the battery's flexibility and applicability, promoting better contact with electrode materials, forming a stable interface, reducing internal resistance, and improving energy density and cycle life. Aqueous electrolytes have garnered significant attention due to their safety profile and the potential for a theoretically longer cycle life in aqueous ZIBs. Table 2 records the chemical performance comparison of $ZnSO_4$, $MnSO_4$ and $Zn(CF_3SO_3)_2$, which can also be applied to ZMBs. Notably, gel electrolytes have emerged as a widely adopted choice for ZMBs, imparting substantial enhancements to battery performance[130]. A gel electrolyte is crafted through the cross-linked polymerization of organic electrolytes, endowing it with a stable network structure, commendable mechanical strength[131], and flexibility[132]. This electrolyte exhibits excellent adaptability in practical applications, furnishing an effective conduit for Zn^{2+} transmission while concurrently enhancing Zn^{2+} mobility[133].

Gel electrolytes not only enhance battery safety and stability but also contribute to more efficient energy storage and prolonged service life. For instance, Liu et al. developed a PVA-$Zn(CF_3SO_3)_2$-TiO_2 network gel electrolyte with high ionic conductivity and transport kinetics by incorporating a TiO_2 precursor through MXene (as depicted in Figure 9)[151]. In Zn//Zn symmetrical batteries, this electrolyte demonstrated a stable cycle time of over 3,000 hours. The network structure of the gel electrolyte promotes the uniform arrangement of TiO_2 nanosheets. The addition of TiO_2 creates a Zn^{2+} migration path on the surface, reduces polymer crystallinity, enhances the mechanical properties and ionic conductivity of the gel electrolyte, and optimizes the effect of promoting Zn^{2+} transport. Additionally, the presence of numerous side hydroxy groups and hydrogen bonds between PVA chains and TiO_2 nanoparticles imparts an autonomous repair function to the prepared gel, thereby improving the stability and cycle life of the battery.

The tetrahedral coordination of Zn^{2+} enables faster ion movement by transitioning from an unfavorable coordination at the stable site to a more favorable coordination in the activated state. To address ligand resistance in Zn^{2+} transport, constructing a hydrophilic-hydrophobic structure in the gel proves to be an effective method. For instance, Zhao et al.,[152] designed a gel electrolyte incorporating a hydrophilic-hydrophobic layer Zn(AOT)$_2$. The AOT anion in $Zn(AOT)_2$ is a classic amphipathic anion with abundant head groups, featuring hydrophilic sites and two distant hydrophobic tails (Figure 10(a)). The gel forms a layered structure supported by long-range van der Waals attraction through ion-dipole interactions with water molecules (Figure 10(b)). The interlayers consist of Zn-philic AOT anionic heads, facilitating the transport of Zn^{2+}. This gel electrolyte is rate-tolerant, supporting a high current density of 3 mA·cm^{-2} with an areal capacity of 1.5 mAh·cm^{-2}. The Zn-MnO_2 full battery assembled using this gel electrolyte demonstrates a stable cycle of over 500 cycles and a high charge and discharge efficiency close to 100%.

Table 2 Comparison of electrochemical performance of batteries using Zn foil as anode and various aqueous electrolytes

Electrolyte	Concentration (M)	Capacity	Electrochemical performance	References
$ZnSO_4$	1	270 (100 mA·g^{-1})	75% capacity retention and 100% Coulombic efficiency after more than 200 cycles	[134]
$ZnSO_4$	1	272 (66 mA·g^{-1})	Capacity retention rate of 69% over 50 cycles	[135]
$ZnSO_4$	1	233 (83 mA·g^{-1})	Capacity retention rate of 63% over 50 cycles	[136]
$ZnSO_4$	2	167 (20 mA·cm^{-2})	Capacity retention rate of 88.7% over 10, 000 cycles	[137]
$ZnSO_4$	2	239.2 (100 mA·g^{-1})	Capacity retention rate of 73% over 300 cycles	[138]
$ZnSO_4$	3	66.5 (60 mA·g^{-1})	70% capacity retention after more than 200 cycles	[139]
$ZnSO_4$	3	357 (2.0 A·g^{-1})	Capacity retention rate of 98.5% over 2, 000 cycles	[140]
$ZnSO_4$	3	224 mAh·g^{-1} (100 mA·g^{-1})	Capacity retention rate of 75% over 400 cycles	[141]
$ZnSO_4$/$MnSO_4$	2/0.1	280 mAh·g^{-1} (200 mA·g^{-1})	Capacity retention rate of 40% over 5, 000 cycles	[142]
$ZnSO_4$/$MnSO_4$	2/0.2	382.2 mAh·g^{-1} (300 mA·g^{-1})	Capacity retention is 94% after 3000 cycles at 3 A·g^{-1}	[143]
$ZnSO_4$/$MnSO_4$	2/0.2	290 mAh g^{-1} (90 mA·g^{-1})	Capacity retention rate of 99.9% over 10, 000 cycles	[144]
$Zn(CF_3SO_3)_2$	1	95 mAh·g^{-1} (5 A·g^{-1})	Capacity retention rate is 92% after 3, 000 cycles	[145]
$Zn(CF_3SO_3)_2$	1	180 mAh·g^{-1} (1 A·g^{-1})	Capacity retention rate of 93.3% over 165 cycles	[146]
$Zn(CF_3SO_3)_2$	2	64.7 mAh·g^{-1} (80 mA·g^{-1})	Capacity retention of 95% over 4, 000 cycles at 1 A·g^{-1}	[147]
$Zn(CF_3SO_3)_2$	3	353 mAh·g^{-1} (100 mA·g^{-1})	97% capacity retention after 2, 000 cycles at 5000 mA·g^{-1}	[148]
$Zn(CF_3SO_3)_2$	3	470 mAh·g^{-1} （200 mA·g^{-1})	Capacity retention rate of 91.1% over 4, 000 cycles	[149]
$Zn(CF_3SO_3)_2$	3	381 mAh·g^{-1} (60 mA·g^{-1})	Capacity retention rate of 71% over 900 cycles	[150]

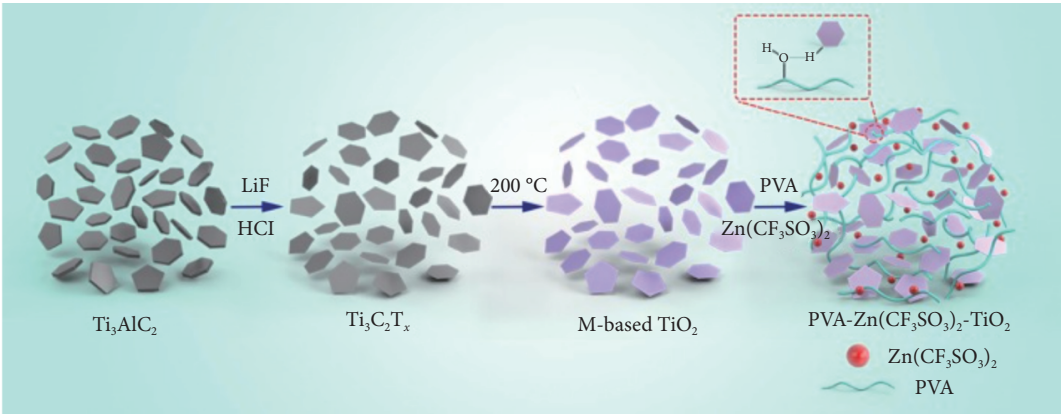

Figure 9 Schematic diagram of preparing TiO_2 gel electrolyte using Ti_3AlC_2 as raw material. Reprinted with permission from Ref. [151], © 2021 Elsevier.

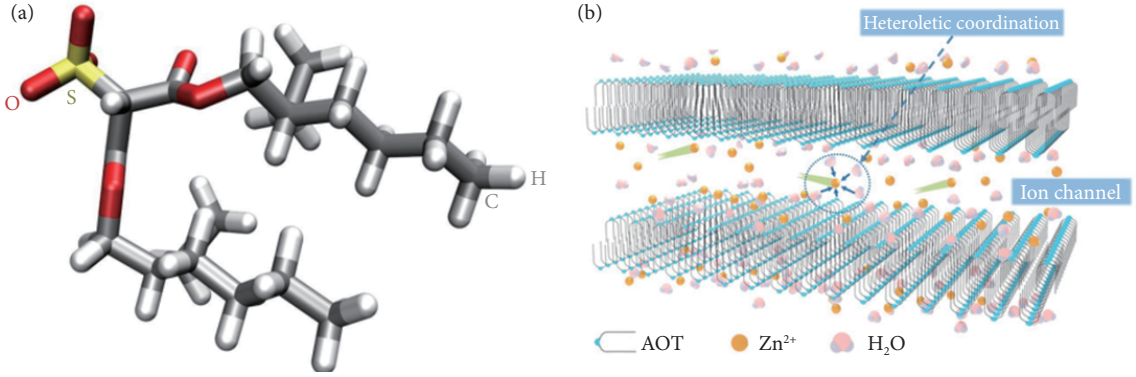

Figure 10 (**a**) Schematic diagram of the AOT anion structure. (**b**) Schematic diagram of $Zn(AOT)_2$ layered structure. Reprinted with permission from Ref. [152], © 2023 Wiley.

The solution to the anode stability problem of ZMBs needs to be achieved through preparation processes. For example, the construction of a three-dimensional porous skeleton anode requires methods such as electrodeposition and bubble methods. Interface engineering also necessitates processes like atomic layer deposition technology and magnetron sputtering to create a protective barrier between the electrode and electrolyte. Following in-depth discussions on anode material selection, porous structure construction, interface engineering at the contact surfaces between the anode and electrolyte as well as between anode materials and current collectors, and electrolyte optimization the stabilization and enhancement of Zn micro-anode performance have been achieved. These advancements are poised to broaden the applications of ZMBs in the realm of new energy, contributing significantly to the advancement of new energy technology in the world.

5 Summary and prospects

ZMBs represent a burgeoning energy storage technology in recent years, yet they grapple with various challenges in practical applications. Through comprehensive research and exploration in this article, we have elucidated numerous effective solutions and improvements. Notably, the utilization of special non-zinc anodes in battery technology has yielded significant enhancements in performance and longevity. Thoughtful selection and design of anode materials, such as zinc oxide and carbon-based materials, play a pivotal role in fortifying battery stability and cycle performance. Furthermore, the application of interface engineering and coating technology optimizes the interaction between the electrode and the electrolyte, thereby enhancing overall battery performance. Of particular significance, the incorporation of gel electrolytes opens up new possibilities for the efficient and stable operation of ZMBs.

ZMBs hold potential applications in various domains: (1) Flexible wearable devices: ZMBs are well-suited for integration into wearable devices like fitness monitors and smartwatches due to their small size and relatively high energy density. (2) Wireless healthcare systems: Applications such as remote heart rate monitors or implantable medical devices, including pacemakers, rely on batteries that can sustain long-term operation while maintaining device portability and mobility. (3) Implantable medical devices: Battery size and weight are critical for implantable devices like neurodetectors and hearing aids to ensure smooth implantation and sustained long-term performance.

With the continuous advancement of science and technology and the expansion of application needs, the research and development of ZMBs still has broad prospects. Future research directions can focus on the following aspects: (1) Material innovation: Continue to explore new anode and electrolyte materials, such as two-dimensional materials, organic-inorganic hybrid materials, etc., to improve the energy density and cycle stability of batteries. (2) Interface engineering: further deepen the research on interface engineering, optimize the interactive interface between electrodes and electrolytes, and reduce energy loss during the battery cycle. (3) Practical application: Verify and test the battery in actual application scenarios to ensure its stability and reliability in complex environments and under high pressure. (4) Sustainability and environmental friendliness: Consider environmental factors during material selection and production processes, and research and develop more environmentally friendly and sustainable battery technologies and production methods. In short, ZMBs are an energy storage technology with great potential, and their future

research and development will make important contributions to global energy transition and sustainable development.

Acknowledgements

This work was supported by the National Key Research Program of China (2022YFE0138100), the National Nature Science Foundation of China (52350710208), the Cooperation Foundation of Yulin University and Dalian National Laboratory for Clean Energy (YLU-DNL fund 2022011), the National Nature Science Foundation of China (22279140, U20A20252, U21A20102, 62174103), the Innovation Fund Project of Dalian Institute of Chemical Physics (DICP I202025, DICP I202032), the Cooperation Foundation of Dalian National Laboratory for Clean Energy of the Chinese Academy of Sciences (DNL202015), the Natural Science Foundation of Liaoning Province (2021-MS-016), the Youth Science and Technology Star Project of Dalian (2021RQ121), the 111 Project (B1404), the Project of Knowledge Innovation Engineering (Y261261606), the Fundamental Research Funds for the Central Universities (GK202103106) and the Shanxi Science and Technology Department (20201101012).

Article history

Received: 23 January 2024; Revised: 20 February 2024; Accepted: 27 February 2024

Additional information

Declaration of competing interest

The authors have no competing interests to declare that are relevant to the content of this article.

References

[1] Pao, H. T., Li, Y. Y., Fu, U. H. C. (2014). Clean energy, non-clean energy, and economic growth in the MIST countries. *Energy Policy*, 67: 932–942.

[2] Olabi, A. G. (2017). Renewable energy and energy storage systems. *Energy*, 136: 1–6.

[3] Ryu, H., Yoon, H. J., Kim, S. W. (2019). Hybrid energy harvesters: Toward sustainable energy harvesting. *Advanced Materials*, 31: 1802898.

[4] Sadorsky, P. (2021). Wind energy for sustainable development: Driving factors and future outlook. *Journal of Cleaner Production*, 289: 125779.

[5] Chowdhury, M. S., Rahman, K. S., Selvanathan, V., Nuthammachot, N., Suklueng, M., Mostafaeipour, A., Habib, A., Akhtaruzzaman, M., Amin, N., Techato, K. (2021). Current trends and prospects of tidal energy technology. *Environment, Development and Sustainability*, 23: 8179–8194.

[6] Kabir, E., Kumar, P., Kumar, S., Adelodun, A. A., Kim, K. H. (2018). Solar energy: Potential and future prospects. *Renewable and Sustainable Energy Reviews*, 82: 894–900.

[7] Yang, Y. S. (2020). A review of electrochemical energy storage researches in the past 22 years. *Journal of Electrochemistry*, 26(4): 443–463. (in Chinese)

[8] Mackanic, D. G., Chang, T. H., Huang, Z., Cui, Y., Bao, Z. (2020). Stretchable electrochemical energy storage devices. *Chemical Society Reviews*, 49: 4466–4495.

[9] Liu, J., Yue, M., Wang, S., Zhao, Y., Zhang, J. (2022). A review of performance attenuation and mitigation strategies of lithium-ion batteries. *Advanced Functional Materials*, 32: 2107769.

[10] Fang, G., Zhou, J., Pan, A., Liang, S. (2018). Recent advances in aqueous zinc-ion batteries. *ACS Energy Letters*, 3: 2480–2501.

[11] Xu, W., Wang, Y. (2019). Recent progress on zinc-ion rechargeable batteries. *Nano-Micro Letters*, 11: 90.

[12] Zhang, N., Chen, X., Yu, M., Niu, Z., Cheng, F., Chen, J. (2020). Materials chemistry for rechargeable zinc-ion batteries. *Chemical Society Reviews*, 49: 4203–4219.

[13] Luc, P. M., Bauer, S., Kowal, J. (2022). Reproducible production of lithium-ion coin cells. *Energies*, 15: 7949.

[14] Bi, S., Wan, F., Wang, S., Jia, S., Tian, J., Niu, Z. (2021). Flexible and tailorable quasi-solid-state rechargeable Ag/Zn microbatteries with high performance. *Carbon Energy*, 3: 167–175.

[15] Wang, X., Wu, Z. S. (2020). Zinc based micro-electrochemical energy storage devices: Present status and future perspective. *EcoMat*, 2: e12042.

[16] Ma, J., Quhe, R., Zhang, W., Yan, Y., Tang, H., Qu, Z., Cheng, Y., Schmidt, O. G., Zhu, M. (2023). Zn microbatteries explore ways for integrations in intelligent systems. *Small*, 19: 2300230.

[17] He, P., Chen, Q., Yan, M., Xu, X., Zhou, L., Mai, L., Nan, C. W. (2019). Building better zinc-ion batteries: A materials perspective. *EnergyChem*, 1: 100022.

[18] Jia, H., Qiu, M., Tang, C., Liu, H., Fu, S., Zhang, X. (2022). Nanoscale BN interface for ultra-stable and wide temperature range tolerable Zn anode. *EcoMat*, 4: e12190.

[19] Zheng, J., Huang, Z., Zeng, Y., Liu, W., Wei, B., Qi, Z., Wang, Z., Xia, C., Liang, H. (2022). Electrostatic shielding regulation of magnetron sputtered Al-based alloy protective coatings enables highly reversible zinc anodes. *Nano Letters*, 22: 1017–1023.

[20] Wang, K., Zhang, X., Han, J., Zhang, X., Sun, X., Li, C., Liu, W., Li, Q., Ma, Y. (2018). High-performance cable-type flexible rechargeable Zn battery based on MnO_2@CNT fiber microelectrode. *ACS Applied Materials & Interfaces*, 10: 24573–24582.

[21] Li, M., Meng, J., Li, Q., Huang, M., Liu, X., Owusu, K. A., Liu, Z., Mai, L. (2018). Finely crafted 3D electrodes for dendrite-free and high-performance flexible fiber-shaped Zn–Co batteries. *Advanced Functional Materials*, 28: 1802016.

[22] Yan, C., Wang, X., Cui, M., Wang, J., Kang, W., Foo, C. Y., Lee, P. S. (2014). Stretchable silver-zinc batteries based on embedded nanowire elastic conductors. *Advanced Energy Materials*, 4: 130139.

[23] Shin, J., You, J. M., Lee, J. Z., Kumar, R., Yin, L., Wang, J., Shirley Meng, Y. (2016). Deposition of ZnO on bismuth species towards a rechargeable Zn-based aqueous battery. *Physical Chemistry Chemical Physics*, 18: 26376–26382.

[24] Cao, L., Fang, G., Cao, H., Duan, X. (2019). Photopatterning and electrochemical energy storage properties of an on-chip organic radical microbattery. *Langmuir*, 35: 16079–16086.

[25] Sun, P., Li, X., Shao, J., Braun, P. V. (2021). High-performance packaged 3D lithium-ion microbatteries fabricated using imprint lithography. *Advanced Materials*, 33: 2006229.

[26] Cho, S., Jung, W., Jung, G. Y., Eom, K. (2020). High-performance boron-doped silicon micron-rod anode fabricated using a mass-producible lithography method for a lithium ion battery. *Journal of Power Sources*, 454: 227931.

[27] Cebollero, J. A., Lahoz, R., Laguna-Bercero, M. A., Larrea, A. (2017). Tailoring the electrode-electrolyte interface of Solid Oxide Fuel Cells (SOFC) by laser micro-patterning to improve their electrochemical performance. *Journal of Power Sources*, 360: 336–344.

[28] Lai, W., Wang, Y., Lei, Z., Wang, R., Lin, Z., Wong, C. P., Kang, F., Yang, C. (2018). High performance, environmentally benign and integratable Zn//MnO_2microbatteries. *Journal of Materials Chemistry A*, 6: 3933–3940.

[29] Kohler, R., Besser, H., Hagen, M., Ye, J., Ziebert, C., Ulrich, S., Proell, J., Pfleging, W. (2011). Laser micro-structuring of magnetron-sputtered SnO_x thin films as anode material for lithium

ion batteries. *Microsystem Technologies*, 17: 225–232.
[30] Kumar, R., Shin, J., Yin, L., You, J. M., Meng, Y. S., Wang, J. (2017). All-printed, stretchable Zn-Ag_2O rechargeable battery via hyperelastic binder for self-powering wearable electronics. *Advanced Energy Materials*, 7: 1602096.
[31] Wang, X., Zheng, S., Zhou, F., Qin, J., Shi, X., Wang, S., Sun, C., Bao, X., Wu, Z. S. (2020). Scalable fabrication of printed Zn//MnO_2 planar micro-batteries with high volumetric energy density and exceptional safety. *National Science Review*, 7: 64–72.
[32] Zhang, Y., Zheng, S., Zhou, F., Shi, X., Dong, C., Das, P., Ma, J., Wang, K., Wu, Z. S. (2022). Multi-layer printable lithium ion micro-batteries with remarkable areal energy density and flexibility for wearable smart electronics. *Small*, 18: 2104506.
[33] Lawes, S., Sun, Q., Lushington, A., Xiao, B., Liu, Y., Sun, X. (2017). Inkjet-printed silicon as high performance anodes for Li-ion batteries. *Nano Energy*, 36: 313–321.
[34] Kolchanov, D. S., Mitrofanov, I., Kim, A., Koshtyal, Y., Rumyantsev, A., Sergeeva, E., Vinogradov, A., Popovich, A., Maximov, M. Y. (2020). Inkjet printing of Li-rich cathode material for thin-film lithium-ion microbatteries. *Energy Technology*, 8: 1901086.
[35] Milroy, C. A., Jang, S., Fujimori, T., Dodabalapur, A., Manthiram, A. (2017). Inkjet-printed lithium–sulfur microcathodes for all-printed, integrated nanomanufacturing. *Small*, 13: 1603786.
[36] Sowade, E., Polomoshnov, M., Willert, A., Baumann, R. R. (2019). Toward 3D-printed electronics: Inkjet-printed vertical metal wire interconnects and screen-printed batteries. *Advanced Engineering Materials*, 21: 1900568.
[37] Sun, K., Wei, T. S., Ahn, B. Y., Seo, J. Y., Dillon, S. J., Lewis, J. A. (2013). 3D printing of interdigitated Li-ion microbattery architectures. *Advanced Materials*, 25: 4539–4543.
[38] Cao, D., Xing, Y., Tantratian, K., Wang, X., Ma, Y., Mukhopadhyay, A., Cheng, Z., Zhang, Q., Jiao, Y., Chen, L., et al. (2019). 3D printed high-performance lithium metal microbatteries enabled by nanocellulose. *Advanced Materials*, 31: 1807313.
[39] Wang, R., Zhang, Y., Xi, W., Zhang, J., Gong, Y., He, B., Wang, H., Jin, J. (2023). 3D printing of hierarchically micro/nanostructured electrodes for high-performance rechargeable batteries. *Nanoscale*, 15: 13932–13951.
[40] Ma, J., Zheng, S., Chi, L., Liu, Y., Zhang, Y., Wang, K., Wu, Z. S. (2022). 3D printing flexible sodium-ion microbatteries with ultrahigh areal capacity and robust rate capability. *Advanced Materials*, 34: 2205569.
[41] Zhou, L., Ning, W., Wu, C., Zhang, D., Wei, W., Ma, J., Li, C., Chen, L. (2019). 3D-printed microelectrodes with a developed conductive network and hierarchical pores toward high areal capacity for microbatteries. *Advanced Materials Technologies*, 4: 1800402.
[42] Zhang, F., Wei, M., Viswanathan, V. V., Swart, B., Shao, Y., Wu, G., Zhou, C. (2017). 3D printing technologies for electrochemical energy storage. *Nano Energy*, 40: 418–431.
[43] Chang, P., Mei, H., Zhou, S., Dassios, K. G., Cheng, L. (2019). 3D printed electrochemical energy storage devices. *Journal of Materials Chemistry A*, 7: 4230–4258.
[44] Tian, X., Jin, J., Yuan, S., Chua, C. K., Tor, S. B., Zhou, K. (2017). Emerging 3D-printed electrochemical energy storage devices: A critical review. *Advanced Energy Materials*, 7: 1700127.
[45] Gao, X., Liu, K., Su, C., Zhang, W., Dai, Y., Parkin, I. P., Carmalt, C. J., He, G. (2024). From bibliometric analysis: 3D printing design strategies and battery applications with a focus on zinc-ion batteries. *SmartMat*, 5: e1197.
[46] Wu, B., Guo, B., Chen, Y., Mu, Y., Qu, H., Lin, M., Bai, J., Zhao, T., Zeng, L. (2023). High zinc utilization aqueous zinc ion batteries enabled by 3D printed graphene arrays. *Energy Storage Materials*, 54: 75–84.
[47] Gao, W., Michalička, J., Pumera, M. (2022). Hierarchical atomic layer deposited V_2O_5 on 3D printed nanocarbon electrodes for high-performance aqueous zinc-ion batteries. *Small*, 18: 2105572.
[48] Kalkal, A., Kumar, S., Kumar, P., Pradhan, R., Willander, M., Packirisamy, G., Kumar, S., Malhotra, B. D. (2021). Recent advances in 3D printing technologies for wearable (bio)sensors. *Additive Manufacturing*, 46: 102088.
[49] Shi, H., Cao, J., Sun, Z., Ali Ghazi, Z., Zhu, X., Han, S., Ren, D., Lu, G., Lan, H., Li, F. (2023). 3D printing enables customizable batteries. *Batteries & Supercaps*, 6: 2300161.
[50] Zhu, C., Schorr, N. B., Qi, Z., Wygant, B. R., Turney, D. E., Yadav, G. G., Worsley, M. A., Duoss, E. B., Banerjee, S., Spoerke, E. D., et al. (2023). Direct ink writing of 3D Zn structures as high-capacity anodes for rechargeable alkaline batteries. *Small Structures*, 4: 2200323.
[51] Liu, G., Ma, Z., Li, G., Yu, W., Wang, P., Meng, C., Guo, S. (2023). All-printed 3D solid-state rechargeable zinc-air microbatteries. *ACS Applied Materials & Interfaces*, 15: 13073–13085.
[52] Ma, H., Tian, X., Fan, J., Cao, W., Yuan, X., Hou, S., Jin, H. (2022). 3D printing of solid-state zinc-ion microbatteries with ultrahigh capacity and high reversibility for wearable integration design. *Journal of Power Sources*, 550: 232152.
[53] Lacey, S. D., Kirsch, D. J., Li, Y., Morgenstern, J. T., Zarket, B. C., Yao, Y., Dai, J., Garcia, L. Q., Liu, B., Gao, T., et al. (2018). Extrusion-based 3D printing of hierarchically porous advanced battery electrodes. *Advanced Materials*, 30: 1705651.
[54] Lu, H., Hu, J., Zhang, K., Zhao, J., Deng, S., Li, Y., Xu, B., Pang, H. (2024). Microfluidic-assisted 3D printing zinc powder anode with 2D conductive MOF/MXene heterostructures for high-stable zinc–organic battery. *Advanced Materials*, 36: 2309753.
[55] Wisnieff, R. (1998). Printing screens. *Nature*, 394: 225–227.
[56] Abdolhosseinzadeh, S., Schneider, R., Verma, A., Heier, J., Nüesch, F., Zhang, C. J. (2020). Turning trash into treasure: Additive free MXene sediment inks for screen-printed micro-supercapacitors. *Advanced Materials*, 32: 2000716.
[57] He, P., Cao, J., Ding, H., Liu, C., Neilson, J., Li, Z., Kinloch, I. A., Derby, B. (2019). Screen-printing of a highly conductive graphene ink for flexible printed electronics. *ACS Applied Materials & Interfaces*, 11: 32225–32234.
[58] Niu, H., Liu, Y., Song, H., Meng, Q., Du, Y., Shen, S. Z. (2021). Facile preparation of flexible all organic PEDOT: PSS/methyl cellulose thermoelectric composite film by a screen printing process. *Synthetic Metals*, 276: 116752.
[59] Zeng, J., Dong, L., Sun, L., Wang, W., Zhou, Y., Wei, L., Guo, X. (2021). Printable zinc-ion hybrid micro-capacitors for flexible self-powered integrated units. *Nano-Micro Letters*, 13: 19.
[60] Houle, F. A. (1986). Basic mechanisms in laser etching and deposition. *Applied Physics A Solids and Surfaces*, 41: 315–330.
[61] Li, X., Jin, X., Wang, Y., Zhang, X., Li, D., Wang, J., Yuan, M., Liu, J., Zhao, Y. (2023). All-direct laser patterning zinc-based microbatteries. *Advanced Functional Materials*, https://doi.org/10.1002/adfm.202314060.
[62] Shi, J., Wang, S., Chen, X., Chen, Z., Du, X., Ni, T., Wang, Q., Ruan, L., Zeng, W., Huang, Z. (2019). An ultrahigh energy density quasi-solid-state zinc ion microbattery with excellent flexibility and thermostability. *Advanced Energy Materials*, 9: 1901957.
[63] Wang, Y., Hong, X., Guo, Y., Zhao, Y., Liao, X., Liu, X., Li, Q., He, L., Mai, L. (2020). Wearable textile-based Co–Zn alkaline microbattery with high energy density and excellent reliability. *Small*, 16: 2000293.
[64] Wang, C., Yu, F., Chen, C., Xia, J, H., Gan, Y., Li, J, Y., Yao, J., Zheng, J, J., Chen, X., Wu, Z. et al. (2024). Laser etching of on-chip ultra-high stability flexible micro MnO_2//Zn batteries. *Materials Today Energy*, 41: 101530.
[65] Kim, S., Kim, J., Joung, Y. H., Ahn, S., Choi, J., Koo, C. (2019). Optimization of selective laser-induced etching (SLE) for fabrication of 3D glass microfluidic device with multi-layer micro channels. *Micro and Nano Systems Letters*, 7: 15.
[66] Pu, J., Shen, Z., Zhong, C., Zhou, Q., Liu, J., Zhu, J., Zhang, H. (2020). Electrodeposition technologies for Li-based batteries: New frontiers of energy storage. *Advanced Materials*, 32: 1903808.
[67] Lincot, D. (2005). Electrodeposition of semiconductors. *Thin Solid Films*, 487: 40–48.

[68] Walter, E. C., Zach, M. P., Favier, F., Murray, B. J., Inazu, K., Hemminger, J. C., Penner, R. M. (2003). Metal nanowire arrays by electrodeposition. *ChemPhysChem*, 4: 131–138.
[69] Bicelli, L. P., Bozzini, B., Mele, C., D'Urzo, L. (2008). A review of nanostructural aspects of metal electrodeposition. *International Journal of Electrochemical Science*, 3: 356–408.
[70] Sun, G., Jin, X., Yang, H., Gao, J., Qu, L. (2018). An aqueous Zn–MnO_2 rechargeable microbattery. *Journal of Materials Chemistry A*, 6: 10926–10931.
[71] Wang, H., Guo, R., Li, H., Wang, J., Du, C., Wang, X., Zheng, Z. (2022). 2D metal patterns transformed from 3D printed stamps for flexible Zn//MnO_2 in-plane micro-batteries. *Chemical Engineering Journal*, 429: 132196.
[72] Dai, C., Hu, L., Jin, X., Wang, Y., Wang, R., Xiao, Y., Li, X. Y., Zhang, X. Q., Song, L., Han, H. et al. (2022). Fast constructing polarity-switchable zinc-bromine microbatteries with high areal energy density. *Science Advances*, 8: eabo6688.
[73] Zeng, L., He, H., Chen, H., Luo, D., He, J., Zhang, C. (2022). 3D printing architecting reservoir-integrated anode for dendrite-free, safe, and durable Zn batteries. *Advanced Energy Materials*, 12: 2103708.
[74] Yang, Q., Li, Q., Liu, Z., Wang, D., Guo, Y., Li, X., Tang, Y., Li, H., Dong, B., Zhi, C. (2020). Dendrites in Zn-based batteries. *Advanced Materials*, 32: 2001854.
[75] He, H., Liu, J. (2020). Suppressing Zn dendrite growth by molecular layer deposition to enable long-life and deeply rechargeable aqueous Zn anodes. *Journal of Materials Chemistry A*, 8: 22100–22110.
[76] Zhang, Y., Peng, C. G., Zhang, Y., Yang, S., Zeng, Z., Zhang, X., Qie, L., Zhang, L., Wang, Z. (2022). In-situ crosslinked Zn^{2+}-conducting polymer complex interphase with synergistic anion shielding and cation regulation for high-rate and dendrite-free zinc metal anodes. *Chemical Engineering Journal*, 448: 137653.
[77] Zhang, Q., Luan, J., Huang, X., Zhu, L., Tang, Y., Ji, X., Wang, H. (2020). Simultaneously regulating the ion distribution and electric field to achieve dendrite-free Zn anode. *Small*, 16: 2000929.
[78] Lu, Z., Liang, Q., Wang, B., Tao, Y., Zhao, Y., Lv, W., Liu, D., Zhang, C., Weng, Z., Liang, J., et al. (2019). Graphitic carbon nitride induced micro-electric field for dendrite-free lithium metal anodes. *Advanced Energy Materials*, 9: 1803186.
[79] Zhu, K. P., Guo, C., Gong, W. B., Xiao, Q. H., Yao, Y. G., Davey, K., Wang, Q. H., Mao, J. F., Xue, P., Guo, Z. (2023). Engineering an electrostatic field layer for high-rate and dendrite-free Zn metal anodes. *Energy & Environmental Science*, 16: 3612–3622.
[80] Han, D., Wu, S., Zhang, S., Deng, Y., Cui, C., Zhang, L., Long, Y., Li, H., Tao, Y., Weng, Z., et al. (2020). A corrosion-resistant and dendrite-free zinc metal anode in aqueous systems. *Small*, 16: 2001736.
[81] Fu, J., Cano, Z. P., Park, M. G., Yu, A., Fowler, M., Chen, Z. (2017). Electrically rechargeable zinc–air batteries: Progress, challenges, and perspectives. *Advanced Materials*, 29: 201604685.
[82] He, P., Huang, J. (2022). Chemical passivation stabilizes Zn anode. *Advanced Materials*, 34: 2109872.
[83] Liu, S., Lin, H., Song, Q., Zhu, J., Zhu, C. (2023). Anti-corrosion and reconstruction of surface crystal plane for Zn anodes by an advanced metal passivation technique. *Energy & Environmental Materials*, 6: 12405.
[84] Cabot, P. L., Cortes, M., Centellas, F., Perez, E. (1993). Potentiostatic passivation of zinc in alkaline solutions. *Journal of Applied Electrochemistry*, 23: 371–378.
[85] Zhang, J. Y., Zhu, X. L., Zhang, S. H., Cheng, M., Yu, M. X., Wang, G. W., Li, C. Y. (2019). Selective production of para-xylene and light olefins from methanol over the mesostructured Zn–Mg–P/ZSM-5 catalyst. *Catalysis Science & Technology*, 9: 316–326.
[86] Qiu, D., Li, B., Zhao, C., Dang, J., Chen, G., Qiu, H., Miao, H. (2023). A review on zinc electrodes in alkaline electrolyte: Current challenges and optimization strategies. *Energy Storage Materials*, 61: 102903.
[87] Nie, C., Wang, G., Wang, D., Wang, M., Gao, X., Bai, Z., Wang, N., Yang, J., Xing, Z., Dou, S. (2023). Recent progress on Zn anodes for advanced aqueous zinc-ion batteries. *Advanced Energy Materials*, 13: 2300606.
[88] Yi, Z., Chen, G., Hou, F., Wang, L., Liang, J. (2021). Strategies for the stabilization of Zn metal anodes for Zn-ion batteries. *Advanced Energy Materials*, 11: 2003065.
[89] Bai, X., Nan, Y., Yang, K., Deng, B., Shao, J., Hu, W., Pu, X. (2023). Zn ionophores to suppress hydrogen evolution and promote uniform Zn deposition in aqueous Zn batteries. *Advanced Functional Materials*, 33: 2307595.
[90] Ma, L., Li, Q., Ying, Y., Ma, F., Chen, S., Li, Y., Huang, H., Zhi, C. (2021). Toward practical high-areal-capacity aqueous zinc-metal batteries: Quantifying hydrogen evolution and a solid-ion conductor for stable zinc anodes. *Advanced Materials*, 33: 2007406.
[91] Dong, N., Zhao, X., Yan, M., Li, H., Pan, H. (2022). Synergetic control of hydrogen evolution and ion-transport kinetics enabling Zn anodes with high-areal-capacity. *Nano Energy*, 104: 107903.
[92] Wang, H., Li, H., Tang, Y., Xu, Z., Wang, K., Li, Q., He, B., Liu, Y., Ge, M., Chen, S., et al. (2022). Stabilizing Zn anode interface by simultaneously manipulating the thermodynamics of Zn nucleation and overpotential of hydrogen evolution. *Advanced Functional Materials*, 32: 2207898.
[93] Salarizadeh, P., Rastgoo-Deylami, M., Askari, M. B. (2022). Electrochemical properties of Ni_3S_2@MoS_2-rGO ternary nanocomposite as a promising cathode for Ni–Zn batteries and catalyst towards hydrogen evolution reaction. *Renewable Energy*, 194: 152–162.
[94] Chen, J., Zhao, W., Jiang, J., Zhao, X., Zheng, S., Pan, Z., Yang, X. (2023). Challenges and perspectives of hydrogen evolution-free aqueous Zn-Ion batteries. *Energy Storage Materials*, 59: 102767.
[95] Wang, H., Zhou, A., Hu, Z., Hu, X., Zhang, F., Song, Z., Huang, Y., Cui, Y., Cui, Y., Li, L., et al. (2024). Toward simultaneous dense zinc deposition and broken side-reaction loops in the Zn//V_2O_5 system. *Angewandte Chemie International Edition*, 63: 2318928.
[96] Ren, J. T., Chen, L., Wang, H. Y., Yuan, Z. Y. (2021). Aqueous rechargeable Zn–N_2 battery assembled by bifunctional cobalt phosphate nanocrystals-loaded carbon nanosheets for simultaneous NH_3 production and power generation. *ACS Applied Materials & Interfaces*, 13: 12106–12117.
[97] Lei, L., Dong, J., Ke, S., Wu, S., Yuan, S. (2023). Porous framework materials for stable Zn anodes in aqueous zinc-ion batteries. *Inorganic Chemistry Frontiers*, 10: 5555–5572.
[98] Liu, H., Zhang, G., Wang, L., Zhang, X., Zhao, Z., Chen, F., Song, L., Duan, H. (2021). Engineering 3D architecture electrodes for high-rate aqueous Zn–Mn microbatteries. *ACS Applied Energy Materials*, 4: 10414–10422.
[99] Meng, H., Ran, Q., Dai, T. Y., Shi, H., Zeng, S. P., Zhu, Y. F., Wen, Z., Zhang, W., Lang, X. Y., Zheng, W. T., et al. (2022). Surface-alloyed nanoporous zinc as reversible and stable anodes for high-performance aqueous zinc-ion battery. *Nano-Micro Letters*, 14: 128.[PubMed]
[100] Ruan, J., Ma, D., Ouyang, K., Shen, S., Yang, M., Wang, Y., Zhao, J., Mi, H., Zhang, P. (2023). 3D artificial array interface engineering enabling dendrite-free stable Zn metal anode. *Nano-Micro Letters*, 15: 37.
[101] Tang, Y., Liu, C., Zhu, H., Xie, X., Gao, J., Deng, C., Han, M., Liang, S., Zhou, J. (2020). Ion-confinement effect enabled by gel electrolyte for highly reversible dendrite-free zinc metal anode. *Energy Storage Materials*, 27: 109–116.
[102] Varzi, A., Mattarozzi, L., Cattarin, S., Guerriero, P., Passerini, S. (2018). 3D porous Cu–Zn alloys as alternative anode materials for Li-ion batteries with superior low *T* performance. *Advanced Energy Materials*, 8: 1701706.
[103] Tian, Y., An, Y., Zhang, B. (2023). Approaching microsized alloy anodes via solid electrolyte interphase design for advanced rechargeable batteries. *Advanced Energy Materials*, 13: 2300123.
[104] Xia, A., Pu, X., Tao, Y., Liu, H., Wang, Y. (2019). Graphene oxide

spontaneous reduction and self-assembly on the zinc metal surface enabling a dendrite-free anode for long-life zinc rechargeable aqueous batteries. *Applied Surface Science*, 481: 852–859.

[105] Fu, H., Shi, C., Li, Z., Nie, J., Yao, S. (2022). Chain-tailed dodecahedron structure derived from Zn/Co-ZIFs/CNTs with excellent rate capability as an anode for lithium-ion batteries. *Journal of Alloys and Compounds*, 904: 164104.

[106] Zawar, S., Akbar, M., Mustafa, G. M., Ali, G., Riaz, S., Atiq, S., Chung, K. Y. (2021). CNTs embedded in layered Zn-doped Co_3O_4 nano-architectures as an efficient hybrid anode material for SIBs. *Journal of Alloys and Compounds*, 867: 158730.

[107] Ma, P. C., Tang, B. Z., Kim, J. K. (2008). Effect of CNT decoration with silver nanoparticles on electrical conductivity of CNT-polymer composites. *Carbon*, 46: 1497–1505.

[108] Zhang, D., Shi, L., Fang, J., Li, X., Dai, K. (2005). Preparation and modification of carbon nanotubes. *Materials Letters*, 59: 4044–4047.

[109] Xia, H., Wang, Y., Lin, J., Lu, L. (2012). Hydrothermal synthesis of MnO_2/CNT nanocomposite with a CNT core/porous MnO_2 sheath hierarchy architecture for supercapacitors. *Nanoscale Research Letters*, 7: 33.

[110] Pantano, A. (2018). Mechanical properties of CNT/polymer. In: *Carbon Nanotube-Reinforced Polymers*. Rafiee R. Ed. Amsterdam: Elsevier.

[111] Liu, X. M., Huang, Z. D., Oh, S. W., Zhang, B., Ma, P. C., Yuen, M. M. F., Kim, J. K. (2012). Carbon nanotube (CNT)-based composites as electrode material for rechargeable Li-ion batteries: A review. *Composites Science and Technology*, 72: 121–144.

[112] Zhao, B., Wang, S., Yu, Q., Wang, Q., Wang, M., Ni, T., Ruan, L., Zeng, W. (2021). A flexible, heat-resistant and self-healable "rocking-chair" zinc ion microbattery based on MXene-TiS_2 (de)intercalation anode. *Journal of Power Sources*, 504: 230076.

[113] Zheng, J., Huang, Z., Ming, F., Zeng, Y., Wei, B., Jiang, Q., Qi, Z., Wang, Z., Liang, H. (2022). Surface and interface engineering of Zn anodes in aqueous rechargeable Zn-ion batteries. *Small*, 18: 2200006.

[114] Zhou, J., Xie, M., Wu, F., Mei, Y., Hao, Y., Li, L., Chen, R. (2022). Encapsulation of metallic Zn in a hybrid MXene/graphene aerogel as a stable Zn anode for foldable Zn-ion batteries. *Advanced Materials*, 34: 2106897.

[115] Ma, H., Tian, X., Wang, T., Hou, S., Jin, H. (2023). Multi-channel engineering of 3D printed zincophilic anodes for ultrahigh-capacity and dendrite-free quasi-solid-state zinc-ion microbatteries. *ACS Applied Materials & Interfaces*, 15: 57049–57058.

[116] Zeng, Y., Pei, Z., Luan, D., Lou, X. W. D. (2023). Atomically dispersed zincophilic sites in N, P-codoped carbon macroporous fibers enable efficient Zn metal anodes. *Journal of the American Chemical Society*, 145: 12333–12341.

[117] He, H., Tong, H., Song, X., Song, X., Liu, J. (2020). Highly stable Zn metal anodes enabled by atomic layer deposited Al_2O_3 coating for aqueous zinc-ion batteries. *Journal of Materials Chemistry A*, 8: 7836–7846.

[118] Liang, P., Yi, J., Liu, X., Wu, K., Wang, Z., Cui, J., Liu, Y., Wang, Y., Xia, Y., Zhang, J. (2020). Highly reversible Zn anode enabled by controllable formation of nucleation sites for Zn-based batteries. *Advanced Functional Materials*, 30: 1908528.

[119] Zuo, Y., Wang, K., Pei, P., Wei, M., Liu, X., Xiao, Y., Zhang, P. (2021). Zinc dendrite growth and inhibition strategies. *Materials Today Energy*, 20: 100692.

[120] Wang, J., Yang, Y., Zhang, Y., Li, Y., Sun, R., Wang, Z., Wang, H. (2021). Strategies towards the challenges of zinc metal anode in rechargeable aqueous zinc ion batteries. *Energy Storage Materials*, 35: 19–46.

[121] Cao, P., Zhou, X., Wei, A., Meng, Q., Ye, H., Liu, W., Tang, J., Yang, J. (2021). Fast-charging and ultrahigh-capacity zinc metal anode for high-performance aqueous zinc-ion batteries. *Advanced Functional Materials*, 31: 2100398.

[122] Zeng, X., Xie, K., Liu, S., Zhang, S., Hao, J., Liu, J., Pang, W. K., Liu, J., Rao, P., Wang, Q., et al. (2021). Bio-inspired design of an *in situ* multifunctional polymeric solid–electrolyte interphase for Zn metal anode cycling at 30 $mA{\cdot}cm^{-2}$ and 30 $mA{\cdot}h{\cdot}cm^{-2}$. *Energy & Environmental Science*, 14: 5947–5957.

[123] Zhai, S., Wang, N., Tan, X., Jiang, K., Quan, Z., Li, Y., Li, Z. (2021). Interface-engineered dendrite-free anode and ultraconductive cathode for durable and high-rate fiber Zn dual-ion microbattery. *Advanced Functional Materials*, 31: 2008894.

[124] He, Y., Pham, H., Liang, X., Park, J. (2022). Impact of ultrathin coating layer on lithium-ion intercalation into particles for lithium-ion batteries. *Chemical Engineering Journal*, 440: 135565.

[125] Jin, Y., Han, K. S., Shao, Y., Sushko, M. L., Xiao, J., Pan, H., Liu, J. (2020). Stabilizing zinc anode reactions by polyethylene oxide polymer in mild aqueous electrolytes. *Advanced Functional Materials*, 30: 2003932.

[126] Zhu, M., Hu, J., Lu, Q., Dong, H., Karnaushenko, D. D., Becker, C., Karnaushenko, D., Li, Y., Tang, H., Qu, Z., et al. (2021). A paternable and *in situ* formed polymeric zinc blanket for a reversible zinc anode in a skin-mountable microbattery. *Advanced Materials*, 33: 2007497.

[127] Zhou, Y., Li, W., Xie, Y., Deng, L., Ke, B., Jian, Y., Cheng, S., Qu, B., Wang, X. (2023). Vertical graphene film enables high-performance quasi-solid-state planar zinc-ion microbatteries. *ACS Applied Materials & Interfaces*, 15: 9486–9493.

[128] Ye, Z., Cao, Z., Lam Chee, M. O., Dong, P., Ajayan, P. M., Shen, J., Ye, M. (2020). Advances in Zn-ion batteries via regulating liquid electrolyte. *Energy Storage Materials*, 32: 290–305.

[129] Liu, D., Tang, Z., Luo, L., Yang, W., Liu, Y., Shen, Z., Fan, X. H. (2021). Self-healing solid polymer electrolyte with high ion conductivity and super stretchability for all-solid zinc-ion batteries. *ACS Applied Materials & Interfaces*, 13: 36320–36329.

[130] Qi, R., Tang, W., Shi, Y., Teng, K., Deng, Y., Zhang, L., Zhang, J., Liu, R. (2023). Gel polymer electrolyte toward large-scale application of aqueous zinc batteries. *Advanced Functional Materials*, 33: 2306052.

[131] Fu, C., Wang, Y., Lu, C., Zhou, S., He, Q., Hu, Y., Feng, M., Wan, Y., Lin, J., Zhang, Y., et al. (2022). Modulation of hydrogel electrolyte enabling stable zinc metal anode. *Energy Storage Materials*, 51: 588–598.

[132] Yang, M., Zhu, J., Bi, S., Wang, R., Niu, Z. (2022). A binary hydrate-melt electrolyte with acetate-oriented cross-linking solvation shells for stable zinc anodes. *Advanced Materials*, 34: 2201744.

[133] Lee, C. J., Wu, H., Hu, Y., Young, M., Wang, H., Lynch, D., Xu, F., Cong, H., Cheng, G. (2018). Ionic conductivity of polyelectrolyte hydrogels. *ACS Applied Materials & Interfaces*, 10: 5845–5852.

[134] Islam, S., Alfaruqi, M. H., Mathew, V., Song, J., Kim, S., Kim, S., Jo, J., Baboo, J. P., Pham, D. T., Putro, D. Y., et al. (2017). Facile synthesis and the exploration of the zinc storage mechanism of β-MnO_2 nanorods with exposed (101) planes as a novel cathode material for high performance eco-friendly zinc-ion batteries. *Journal of Materials Chemistry A*, 5: 23299–23309.

[135] Islam, S., Alfaruqi, M. H., Song, J., Kim, S., Pham, D. T., Jo, J., Kim, S., Mathew, V., Baboo, J. P., Xiu, Z., et al. (2017). Carbon-coated manganese dioxide nanoparticles and their enhanced electrochemical properties for zinc-ion battery applications. *Journal of Energy Chemistry*, 26: 815–819.

[136] Alfaruqi, M. H., Gim, J., Kim, S., Song, J., Jo, J., Kim, S., Mathew, V., Kim, J. (2015). Enhanced reversible divalent zinc storage in a structurally stable α-MnO_2 nanorod electrode. *Journal of Power Sources*, 288: 320–327.

[137] Zeng, Y., Zhang, X., Qin, R., Liu, X., Fang, P., Zheng, D., Tong, Y., Lu, X. (2019). Dendrite-free zinc deposition induced by multifunctional CNT frameworks for stable flexible Zn-ion batteries. *Advanced Materials*, 31: 1903675.

[138] Hao, J., Mou, J., Zhang, J., Dong, L., Liu, W., Xu, C., Kang, F. (2018). Electrochemically induced spinel-layered phase transition of Mn_3O_4 in high performance neutral aqueous rechargeable zinc battery. *Electrochimica Acta*, 259: 170–178.

[139] Zhang, L., Chen, L., Zhou, X., Liu, Z. (2015). Morphology-dependent electrochemical performance of zinc hexacyanoferrate cathode for zinc-ion battery. *Scientific Reports*, 5: 18263.

[140] Dong, Y., Jia, M., Wang, Y., Xu, J., Liu, Y., Jiao, L., Zhang, N. (2020). Long-life zinc/vanadium pentoxide battery enabled by a concentrated aqueous $ZnSO_4$ electrolyte with proton and zinc ion co-intercalation. *ACS Applied Energy Materials*, 3: 11183–11192.

[141] Zhou, J., Shan, L., Wu, Z., Guo, X., Fang, G., Liang, S. (2018). Investigation of V_2O_5 as a low-cost rechargeable aqueous zinc ion battery cathode. *Chemical Communications*, 54: 4457–4460.

[142] Huang, J., Wang, Z., Hou, M., Dong, X., Liu, Y., Wang, Y., Xia, Y. (2018). Polyaniline-intercalated manganese dioxide nanolayers as a high-performance cathode material for an aqueous zinc-ion battery. *Nature Communications*, 9: 2906.

[143] Wu, B., Zhang, G., Yan, M., Xiong, T., He, P., He, L., Xu, X., Mai, L. (2018). Graphene scroll-coated α-MnO_2 nanowires as high-performance cathode materials for aqueous Zn-ion battery. *Small*, 14: 1703850.

[144] Sun, W., Wang, F., Hou, S., Yang, C., Fan, X., Ma, Z., Gao, T., Han, F., Hu, R., Zhu, M., et al. (2017). Zn/MnO_2 battery chemistry with H^+ and Zn^{2+} coinsertion. *Journal of the American Chemical Society*, 139: 9775–9778.

[145] Wan, F., Zhang, L., Wang, X., Bi, S., Niu, Z., Chen, J. (2018). An aqueous rechargeable zinc-organic battery with hybrid mechanism. *Advanced Functional Materials*, 28: 1804975.

[146] Qin, H., Yang, Z., Chen, L., Chen, X., Wang, L. (2018). A high-rate aqueous rechargeable zinc ion battery based on the VS_4@rGO nanocomposite. *Journal of Materials Chemistry A*, 6: 23757–23765.

[147] Li, W., Wang, K., Cheng, S., Jiang, K. (2018). A long-life aqueous Zn-ion battery based on $Na_3V_2(PO4)_2F_3$ cathode. *Energy Storage Materials*, 15: 14–21.

[148] Ming, F., Liang, H., Lei, Y., Kandambeth, S., Eddaoudi, M., Alshareef, H. N. (2018). Layered $Mg_xV_2O_5{\cdot}nH_2O$ as cathode material for high-performance aqueous zinc ion batteries. *ACS Energy Letters*, 3: 2602–2609.

[149] Zhang, N., Dong, Y., Jia, M., Bian, X., Wang, Y., Qiu, M., Xu, J., Liu, Y., Jiao, L., Cheng, F. (2018). Rechargeable aqueous $Zn–V_2O_5$ battery with high energy density and long cycle life. *ACS Energy Letters*, 3: 1366–1372.

[150] Yan, M., He, P., Chen, Y., Wang, S., Wei, Q., Zhao, K., Xu, X., An, Q., Shuang, Y., Shao, Y., et al. (2018). Water-lubricated intercalation in $V_2O_5{\cdot}nH_2O$ for high-capacity and high-rate aqueous rechargeable zinc batteries. *Advanced Materials*, 30: 1703725.

[151] Liu, C., Tian, Y., An, Y., Yang, Q., Xiong, S., Feng, J., Qian, Y. (2022). Robust and flexible polymer/MXene-derived two dimensional TiO_2 hybrid gel electrolyte for dendrite-free solid-state zinc-ion batteries. *Chemical Engineering Journal*, 430: 132748.

[152] Zhao, Z., Nian, B., Lei, Y., Wang, Y., Shi, L., Yin, J., Mohammed, O. F., Alshareef, H. N. (2023). A novel plastic-crystal electrolyte with fast ion-transport channels for solid zinc-ion batteries. *Advanced Energy Materials*, 13: 2300063.